X-RAY DIFFRACTION STUDIES OF DEOXYRIBONUCLEOHISTONE

by

William Slate Wilson, B.A.

A THESIS
Presented to the Department of Anatomy
and the Graduate Division of the University of Oregon Medical School
in partial fulfillment of
the requirements for the degree of
Master of Science

June 1964

APPROVE [redacted]

. . . . . .

(Professor in Charge of Thesis)

[redacted]

. . . . . .

(Chairman, Graduate Council)

ACKNOWLEDGEMENTS

There are many people to whom I am greatly indebted for help along the way to completion of this thesis. First to a pair of tolerant parents and very tolerant cousins, Mr. and Mrs. Webb W. Trimble, with whom I lived on my various jaunts to Seattle for diffraction, I would like to express my gratitude. To Dr. Lyle Jensen, Professor of Anatomy at the University of Washington I owe the entire project, for he provided both diffraction equipment and advice. Dr. Robert L. Bacon, my chief, is a very brave man; he had the fortitude to let me work in a field with which he is not familiar. For his willingness to do this and for his constant support during my floundering period I thank him very much.

During the summer of 1963 I spent some time in Dr. David R. Davies laboratory at the National Institutes of Health. Here I learned much about the theory of fiber diffraction, and with his material I obtained my DNA photographs. Also Dr. H. Catherine W. Skinner and Dr. V. Sasisekharan working in this laboratory have been of great help in diffracting some nucleohistone for me.

Finally I would like to thank Dr. Clarissa Beatty at the Oregon Primate Center for running the microkjeldal determinations.

TABLE OF CONTENTS

INTRODUCTION AND REVIEW OF LITERATURE

In the past ten years there has been a remarkable gain in knowledge of the cellular processes leading to protein synthesis. A vitally important piece of information, coming in 1953, was the Watson-Crick[34] molecular model for DNA, which followed the work of Pauling and Corey[26] in 1951 in which they elucidated the alpha-helix. Both of these pieces of work involved a careful consideration of bond angles and distances already known.

Hiatuses, however, remain in the knowledge concerning the regulation of the rate of RNA and protein synthesis and the type of cellular products produced. It has been the author's purpose to study one of these metabolic regulating substances, namely the histones in their attachment to the DNA helix in an attempt to clarify the nature of this bonding.

It has been known for many years that chromosomes contained much more than deoxyribonucleic acid. One of the more recent determinations of the contents of chromosomes, done by Huang and Bonner[14] in 1962, showed that for pea embryo chromatin, the analysis was:

DNA	31%
Histone	33%
RNA	17%
Non-histone protein	18%

In 1951 Mirsky and Ris[21] found that the relative contents of DNA and histone in interphase chromosomes of the cells of calf liver, thymus and kidney was constant, the total amount of histone depending on the total amount of DNA. However, there was no relationship between amounts of DNA and non-histone protein, the latter apparently being directly proportional to the amount of cytoplasm in the cells studied. In this same paper they presented excellent evidence that the histone was bound to

the DNA, for histone blocked Feulgen staining with crystal violet, which combines with DNA deoxyribose groups. The basic substance salmin was found to displace histone and combine with DNA. Cruft, Mauritzen and Stedman[9] also found that the nuclei from "corresponding cells of different species contain virtually the same relative amounts of nucleic acids and histones". Their values also show that, with a few exceptions, the relative amounts of nucleic acid and histone are fairly constant for all cells. They believe that the histone is attached to the DNA by salt bridges.

These experiments led Wilkins, Zubay and Wilson[38] to suspect that the important substance of the chromosomes in somatic cells was the combination of the two, the nucleohistone (or DNH). It should be noted here, however, that Mirsky and Ris[21] found histone can be removed from the chromosomes without destroying the microscopic appearance of the chromosomes, whereas removal of DNA or non-histone protein ("residual" protein), results in loss of chromosomal morphology. In 1959 Wilkins, Zubay and Wilson[38] [39] published two articles on the structure of nucleohistone, determined by x-ray diffraction studies and some model building. Their x-ray diffraction photographs were of poor quality, giving basically a DNA pattern, and, thus, their ideas of structure were admittedly speculative. From their photographs they were unable to tell just how and where the histone was attached to the DNA, but they postulated that it might be in the large grooves and that it was in a typical α-helical structure. Frequent breaks in α-helical axis allowed the histone to coil around the DNA helix. Further, they believed that a 35Å semimeridional arc (from the oriented DNH fibers)

was generated by diffraction from histone bridges "formed between roughly parallel DNA molecules". These bridges were thought to be labile since Zubay and Doty[40] had shown that, in aqueous suspension of concentration less than 0.1%, nucleohistone aggregates break down into single molecules or strands. In concentrations greater than 0.1% nucleohistone aggregates, a phenomenon which does not occur with DNA. The "semimeridional" arc corresponds to diffraction along the fiber length (helix axis), as will be shown in the theoretical discussion of diffraction from α-helices.

Since 35Å is quite close to the value for the DNA pitch length (34Å), Wilkins et al[38] believed that these bridges were formed between the parallel DNA molecules at each turn of the helix. In 1956 Wilkins[35] had reported the finding of a 38Å ring from diffraction photographs of erythrocytic nuclei and thymus chromosomes of about the same intensity as the 35Å. Thus, these authors equated the 35Å arc from fibers with the 38Å ring in the chromosomes and erythrocytes, accounting for the difference of 3Å by suggesting that the two DNA molecules are "bent slightly and coiled around each other in a right-handed direction, the bridge points on one molecule coming into register with those on the other". Bridges may then form about 38Å apart. They also considered it possible that stretching of the DNA molecules might occur, contributing to the 3Å difference. Because the 35Å arc is less well oriented than the DNA portion, the fibers were believed to consist of well oriented DNA and poorly oriented histone in the combination discussed above. The authors concluded that these histone-histone links may be responsible for polyteny. Also found was a strong

60Å reflection which was characteristic of nucleohistone regardless of the source, from which they concluded that, since sphingomyelin has the same pattern (strong 60Å reflection), nucleohistone was contaminated with about 3% sphingomyelin bound to the histone.

Wilkins and Zubay[41] in 1962 reported on further experiments involving x-ray diffraction patterns of sheets and lumps of histones. They found that freshly prepared histones gave mainly the α -helical polypeptide structure with diffuse rings at 4.5 and 10Å, the latter being relatively more intense than the former, typical findings for α -helical structure. As these authors had found previously[38], on dehydrating the DNH fibers (in this case reconstituted from DNA and histone preparations) the DNA pattern disappeared, leaving the histone pattern, whereas at high relative humidity the DNA pattern predominates. This phenomenon was interpreted to mean that, when the DNA structure collapses at low relative humidity the polypeptide chains of histone, being rather weakly attached to the PO_4 groups of DNA, orient poorly side by side giving the diffuse 10Å and 4.5Å rings. Histone was considered, contrary to their earlier reports, as a hydrated gel filling the space between the roughly parallel DNA molecules, weakly attached to the phosphate groups, and not "preferentially aligned parallel or perpendicularly to the length of the DNA molecule". No information was given regarding the protein bridges mention in their earlier article, except that they collapsed somewhat. The author wishes to emphasize at this point that Wilkins, Zubay and Wilson used wide angle x-ray diffraction giving them resolution from about 60Å down to about 2Å.

Recently (August 1963) Luzzati and Nicolaieff[20] published an

Figure 1. Model by Luzzati and Nicolaieff of DNH at concentrations of water and DNH.

Open circles represent DNA.
Cross-hatched areas represent histone gel.

excellent article which is in considerable disagreement with Wilkins, Zubay and Wilson. Luzzati and Nicolaieff, by phase diagram analysis of low angle x-ray diffraction photographs of nucleohistone gels (concentration varying from $\sim$ 0.15 to $\sim$ 0.70), have concluded that, at a concentration of 30%, the nucleohistone consists of an equilibrium between the isotropic (unordered) phase and a liquid-crystalline phase in which there exist parallel associations of DNA molecules surrounded by a cylinder of histone. They have found that chick erythrocyte nuclei give the same pattern. These authors obtained resolution between 30 and 150Å. It was suggested by them that in cells, if this biphasic condition exists in active chromosomes, "environmental changes are buffered by...the proportion of the phases", "the change in H_2O concentration and concomitantly the structure of the DNH", being "related to the different functions that DNA has to perform at the various stages of mitotic activity". The figure below shows the proposed structure at various gel concentrations, the small, round, open circles being the DNA.

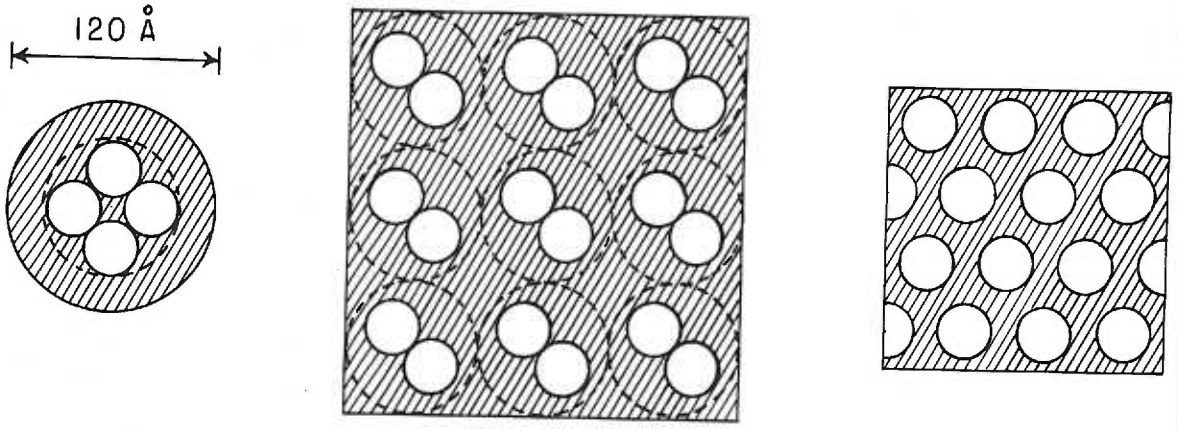

A rather serious limitation to their method, which was recognized by the authors, was the lack of good resolving power. That is, at resolutions only down to 30Å, nothing could be said about the details of bonding between the DNA and the histone or about the actual three-dimensional configuration of the histone itself. It is, consequently, important to attempt to improve upon Wilkins, Zubay and Wilson's fibers and to compare the data at good resolution - down to $\sim$ 2Å.

At this time a general but succinct review of what is known of each of the two components of nucleohistone-DNA and histone is appropriate.

DNA. Watson and Crick[33] in 1953 propounded their now famous molecular structure of DNA. This consisted of a right-handed, two-stranded, coiled (helical) chain of DNA in which the phosphate groups were on the outside and the purine and pyrimidine bases on the inside. The phosphate diester groups joined the β-D-deoxyribofuranose residue through 3'5' linkages, and the sugars were roughly perpendicular to the bases. Purine and pyrimidine base residues were located every 3.4Å along the helix axis, the helical pitch was 34Å, and there was 36° between adjacent base pairs, which meant there were ten base pairs per helical turn. If the most stable form (keto) of the bases was assumed, adenine could hydrogen bond only to thymine and quanine only to cytosine. These hydrogen bonds were thought to occur at purine 1 to pyrimidine 1 and purine 6 to pyrimidine 6 positions. Watson and Crick's x-ray diffraction photographs were not of sufficient quality to check completely with their model, but their model accounted for the finding that adenine:thymine and quanine:cytosine ratios were always very close to unity. The

model, furthermore, was an "open" one and could contain the large amounts of water which had been found experimentally (30%)[34]. Dehydration would result in tipping of the bases to the axis of the helix and a more compact structure - the A-form. The Watson and Crick molecular model was built following scrupulously the known bond angles and bond distances for the small groups of atoms contained within the larger DNA molecules.

Franklin and Gosling[10] and Wilkins,MHF, Stokes and Wilson[37], (in the same issue of "Nature"), substantiated to a great degree the model of Watson and Crick.

Using data obtained from x-ray diffraction of crystals, and hybridization-resonance theory, Pauling and Corey[24] in 1956 reported that whereas adenine-thymine bonding is by two hydrogen bonds, there are three hydrogen bonds between guanine and cytosine. This finding required a slightly different guanine cytosine structure but fitted in quite well with the model of Watson and Crick, and, consequently, modified it only slightly.

Landridge, Wilson, Hooper, Wilkins and Hamilton[19] reported in 1960 that fibers of the lithium salt of DNA were crystalline in the B-form at 66% relative humidity and, therefore, gave many reflections, permitting the Watson-Crick model to be verified completely. Prior to the Li-DNA photographs, fibers of the B-form were not crystallized, and as this was the in vivo form (occurring at higher humidities), it was of importance that this crystalline form was found.

Histones. Histones were defined by Cruft, Mauritzen and Stedman[9] as the basic proteins occurring in the nucleus with the exception of

the protamines. They have an isoelectric point of pH 10-12. In a lengthy review article Phillips[28] discusses the histones. Histones may be divided into three fractions, each of which may be subdivided by various fractional techniques. These three fractions are the very lysine rich, the moderately lysine rich and the arginine rich.

1. Very lysine rich fraction. This fraction, constituting about 15 to 20% of total histone, has a molecular weight of about 10,000 ± 2,000, making it the lightest of the fractions by a considerable amount. It possesses a lysine:arginine ratio of greater than 4. It is the fraction removed most easily from DNA, and it does not aggregate in suspension as do the other two fractions. These two properties are thought to be related to the low arginine content, this amino acid probably being responsible for the strongest salt linkages. The very lysine rich fraction has few aromatic or heterocyclic amino acids to form Van der Waals ring-ring forces, and it has considerably more proline than the other fractions. Amino acid analysis indicates that it contains about 25 mole % lysine, 3 mole % arginine, 0.1-0.4 mole % histidine, 9-14 mole % proline and 8 mole % acidic amino acids (glutamic and aspartic). There seems to be a large quantity of alanine. N-terminal groups are scanty, but the f 1 (b) fraction has approximately 50% N-terminal threonine, according to Butler[6], the other fractions being mainly acetylated in the N-terminal end. It is considered to be the fraction which has the most regular structure, and there is the possibility that it exists as the extended ß-configura-

tion. The basic amino acids are spaced about four residues apart.

2. Moderately lysine rich fraction. The moderately (or slightly) lysine rich fraction holds an intermediate position between the very lysine rich and the arginine rich fractions in many of its properties. It has a lysine:arginine ratio of 1 to 4 and is easier to remove from its complex with DNA than is the arginine rich fraction but more difficult to remove than the very lysine rich. It aggregates more in suspension than does the very lysine rich, less than the arginine rich. This fraction contains about half as much proline as the very lysine rich fraction and probably exists in the α-helix. The significant amino acid analysis is as follows: arginine 8-10 mole %, lysine 11-18 mole %, histidine 0.6-3.0 mole %, proline 3.8-6.0 mole %, acidic amino acids 5.0-14.0 mole %. The f 2 (b) fraction contains 77-97% proline N-terminal groups, whereas the f 2 (a) fraction is mainly acetylated. The structure is less regular than the very lysine rich with the basic amino acids spaced zero to seven residues apart. This fraction constitutes 50% of whole histone.

3. Arginine rich fraction. The arginine fraction of histones is the one which is most tightly bound to DNA since arginine has many opportunities for salt linkages. It accounts for about 20% of whole histone. It aggregates rapidly in suspension. Factors favoring aggregation include high pH, high anion valency, increased concentration and high temperature. The lysine:arginine ratio is

less than unity. The significant amino acid composition is arginine 11-14 mole %, lysine 9-10.3 mole %, histidine 1.9-2.3 mole %, proline 3.0-4.9 mole %, acidic amino acids 15-17 mole %. N-terminal analysis reveals alanine as the N-terminal amino acid 70-96% of the time.

There has been much controversy over whether histones are cell, tissue and/or species specific. A few points in this regard should suffice. Butler,[6] in an article published in September 1963, stated that large differences in the amino acid composition are found in very widely separated species. Wheat germ histones differ markedly from animal histones, the former being higher in lysine content and without an arginine rich fraction. Hnilica, Jones and Butler[13] reported in 1962 on extractions of the three histone fractions from calf thymus, calf liver, calf spleen, rat liver, rat spleen, leukemic rat spleen and Erlish ascites cells. After purification of each fraction by starch gel electrophoresis, these authors stated that no significant differences in amino acid composition and N-terminal groups existed in corresponding fractions from the different sources. No attempt was made to quantitate the percentage of each histone from the individual sources, but the starch gel bands appeared similar on visual examination. Phillips (1957)[28] believes that the specificity, if any, may reside in minor differences of amino acid sequence, for trypsin digestion yielded 35 different peptides from several sources. Sporn and Dingman[30] in 1963, however, reported that in isolated brain and liver nuclei of chicken the ratio of histone to DNA is less than for chicken erythrocytes. Moreover, DNH from the brain and liver nuclei is more soluble in isotonic saline

than is the DNH from chicken erythrocytes. In another recent report, Hidvegi, Arky, Antoni and Varteresz[12] incubated rabbit bone marrow cells with ^{14}C-labeled lysine. They extracted the cells for histone which was then chromatographed in carboxymethycellulose and eluted with 1N and 8N formic acid. It was found that there were nine to ten peaks similar to those reported in 1959 by Busch and Davis[12]. There was one heavily labeled (lysine rich (?)) fraction thought to be the same as Busch and Davis' RP2-L present only in malignant tissues. Hidvégi et al suggested that the presence of this histone fraction, which has a fast turnover, may indicate a rapid turnover in the cells in which it is found in abundance in a consequent "change in metabolic control". These authors believed that this was merely an increase in amount of this fraction, not a new fraction.

Much work has been done in recent years on function of the histone in its relation to DNA. In general, the work on function has been more rewarding than that on structure. Stedman and Stedman[31] in 1950 were among the first to point out that histones might act as suppressors of gene activity. In 1962 Huang and Bonner[14] using pea embryo chromatin found that a suspension of DNA and RNA polymerase produced five times the quantity of RNA as did the crude chromatin.

Allfrey, Littau and Mirsky[1] in an article appearing in 1963 stated inhibition of RNA synthesis by histones probably was"due in part to the fact that histones can inhibit nuclear ATP-dependent 'activation' of amino acids needed for protein synthesis and also diminish the kinase activities and ATP 'pool' required for RNA synthesis" by combining with negatively charged polymers. These authors

found that the degree of inhibition of DNA-dependent RNA synthesis was related to the type of histone added to the medium. The arginine rich fractions were highly inhibitory, and the lysine rich fractions weakly so. Total histone was between the two fractions in its activity. Amino acid uptake by the incubated nuclei was also inhibited more by the arginine rich than the lysine rich fraction, but if alanine - ^{14}C was added to the system before the histone (thus allowing it to enter the nuclei), its incorporation into protein was still inhibited. When trypsin, which has relative preference for bonds involving arginine and lysine, was added to the system, an approximately 70% increase in the uptake by the nuclei of precursors of RNA occurred, as well as a marked increase in RNA synthesis. These authors suggested a model of a chromosome in which much of the DNA is bound to histone which inhibits synthesis of messenger RNA. Active portions of the genes would contain lysine rich fractions, inactive portions would be covered more by the arginine rich fractions.

Bonner and Huang[5], also in 1963, again working with chromatin and nucleohistone from pea embryos, found that the chromatin contained both nucleohistone and uncomplexed DNA. This was thought to be the case since the chromatin exhibited a two step melting profile, the first step having a Tm of 69.5°C (Tm = 70.°C is typical of DNA) and the second step with a Tm of 84.°C (Tm - 84.°C for nucleohistone). When RNA polymerase was added to reaction mixtures of both purified DNA and chromatin, the latter mixture, which contained about five times as much DNA as the former, yielded slightly more than three-fourths the amount of DNA-dependent RNA which the purified DNA produced. The authors, therefore,

concluded that approximately 20% of the DNA in chromatin was uncomplexed with histone.

In 1957 Crick, Griffith and Orgel[7] had reported a mathematical solution with the physical manifestation of a non-overlapping amino acid code without commas, each amino acid being coded by a sequence of three nucleotides (of RNA). This fit experimental findings of an unrestricted sequence of amino acids in polypeptides; there were twenty possible sequences of the nucleotides, corresponding to the twenty amino acids. Bloch[4] in 1962 pointed out that if this code applied to histone and if DNA was the ultimate source of coding of histone, there was obviously insufficient DNA nucleotide for the control of synthesis of the histone associated with it. This was because there were about three to four amino acid histones associated with each DNA nucleotide. Phillips[28] stated that there may be a distance of zero to seven non-basic amino acids between each basic amino acid, depending upon the type of histone. Bloch then deduced that there must be fewer types of histone molecules than their associated nucleotide sequence and different nucleotide sequences must associated with similar histone molecules. He further concluded that at different times a given gene locus will associate with different histones, a scheme which would fit in well with Zubay and Wilkins' most recent ideas as well as with those of Luzzati. Vendrely, Knobloch and Vendrely[32] in 1960 reported quantitative studies of phosphate groups and basic amino acids of histones. They stated that all of the phosphate groups could be saturated with the basic amino acids of histone (arginine, lysine, histidine) but that the actual saturation may vary considerably.

Finally, Izawa, Allfrey and Mirsky[15] in 1963 reported experiments on lampbrush chromosomes, done on *in vitro* preparations of both isolated chromosomes and free oocytes. It was found that (1) the RNA synthesis occurring on the loops was DNA dependent since Actinomycin D, combining selectively with primer DNA, blocks completely RNA synthesis as measured by the uptake of tritiated purines and pyrimidines, (2) the appearance of the loops depended on the synthesis of RNA, and (3) histone, particularly the arginine rich fraction, caused both inhibition of RNA synthesis and retraction of loops, whereas the lysine rich fraction does neither.

It is possible then, in summary, to say that the histones consist of a group of characteristic proteins, not an artifactual or heterogeneous population, which is attached in some manner, specific or non-specific, to the DNA and which may be responsible for the way in which genes are expressed. Also, it may be said that any structure proposed for nucleohistone must account for (1) the RNA inhibition effects of histones with the arginine rich fractions being by far the most inhibitory, (2) the probability that similar histones can combine with different DNA nucleotide sequences, (3) that the histones may shift around in relation to the DNA at different times depending upon the nuclear concentration, both in ionic and of the nucleohistone, (4) that some of the DNA is uncomplexed with histone much of the time, and (5) that the histone be mainly α-helical. The mode of attachment to the DNA molecule, therefore, is of more than academic interest.

The author will now present an exposition of the theory of x-ray diffraction. It should be realized at the outset that minimm of classical

crystallography and rigorous mathematical proofs will be given. In the case of crystallography the concepts will be first discussed in terms of two-dimensional structures; the mathematical proofs given are only those which are of importance. Much explanation of mathematical representations will be given and will, the author hopes, be more meaningful.

The need for x-ray diffraction should first be established, since it may seem to the reader that this is an unseemingly complicated method with which to view the structure of macromolecules. X-ray diffraction is used because it is the one method of viewing macromolecules that is available at present which will allow resolution down to atomic levels. With a 2Å resolution it is possible to place unambiguously all atoms in a molecule. With large molecules, however, and particularly with heterogeneous ones, such resolution is often not possible, but the crystallographer is able to achieve good enough resolution so that, in combination with model building, he is able to arrive at a fairly good structure for the macromolecule.

There is one very severe limitation which is placed upon an x-ray diffraction structure analysis, one which should never be minimized in a proposed analysis, and this is that the material be in a crystalline form. It is a crystallographic axiom that heterogeneous substances will not crystallize; hence it is necessary to purify the material as much as possible, which process, of course, often requires that many different operations be performed on the material. In purifying macromolecules there is always a considerable risk in destroying the native configuration, if not the entire molecule; however, since as little as

a few parts per million of contaminating material will inhibit nucleation and/or crystal growth of organic substances, this risk must be taken.

DNA and the nucleoproteins are such macromolecules, neither of which is homogeneous, and neither of which will, therefore, form large enough crystals for practical use. With both macromolecules, however, it is possible, by drawing out fibers, to force orientation of the roughly cylindrical molecules so that they lie with their long axes parallel and along the fiber axis. Because the homogenous phosphate-deoxyribose backbone of the DNA molecules is located on the outside of the molecule, and the heterogeneous portion of the molecule, the centrally occurring adenine-thymine and guanine-cytosine base pairs are more or less hidden by this homogeneous backbone, DNA fibers will be very nearly crystalline, as noted by the diffraction as sharp spots within the diffuse arcs. However, the heterogeneous base pairs do diffract as a diffuse arc (see photograph of DNA in the section on results). In the case of nucleohistone, however, despite the fact that the histones are a clear cut, well defined group of proteins, they nevertheless are heterogeneous. Since presumably they surround the homogeneous phosphate-deoxyribose backbone, one molecule of DNH does not appear the same as all others (as is the case with DNA); consequently, it cannot be expected that as well-oriented fibers are possible, and there will be few sharp spots (if any) and many arcs or circles. This situation leads to a more ambiguous interpretation of the x-ray diffraction photographs.

Two minimal types of disorientation for structures containing helical molecules has been postulated by Klug and Franklin[18] and are illus-

Figure 2. Illustrates the types of disorder in fibers of polymers.

The lines on the left represent perfect allignment and random displacement along the fiber (helix) axis.

The circles on the right represent rotation disorder, the squares and triangles representing identical portions of the molecules.

trated in figure (2) below. These types of disorder are (1) random

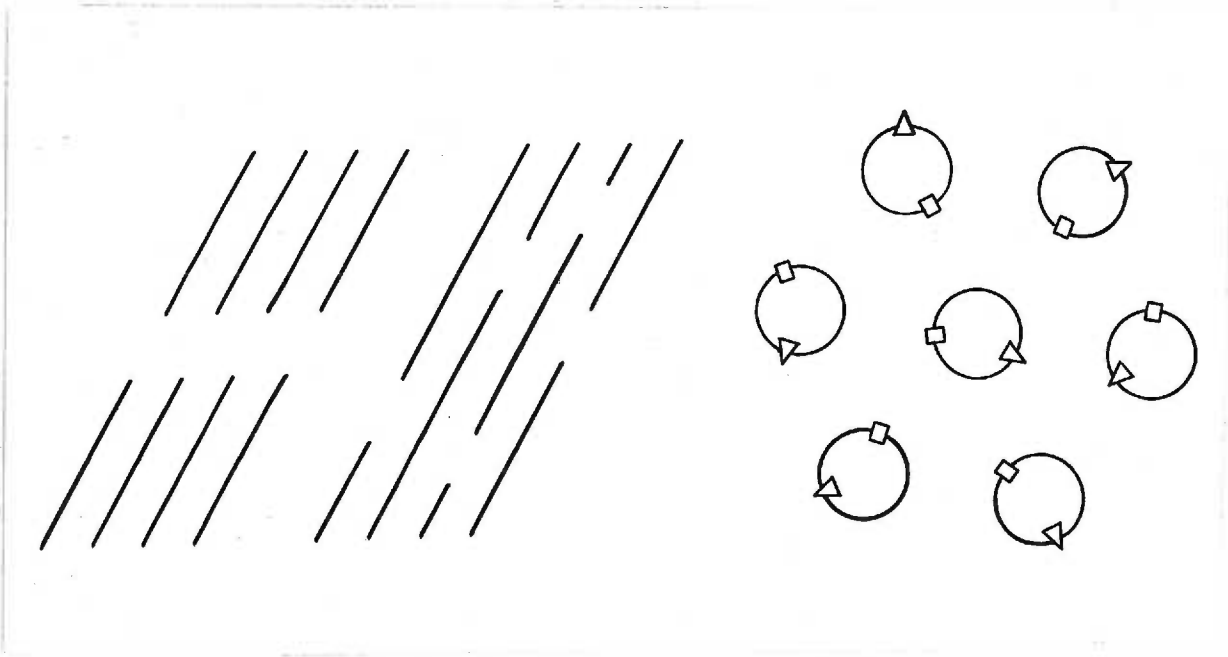

Figure 2.

rotation about the fiber axis as noted in the right-hand portion of the figure, in which the triangle and square are merely markers on identical positions of the molecule, and (2) variable displacement of the helices along their axes with regard to one another. In combination these two types of disorder give rise to a "screw disorder". The combination has been shown by Landridge et al[19] (1960) to exist for DNA. Whether or not this type of fiber disorder exists for DNH is not known since the effect of the histone is not known. Upon these types of disorder will be superimposed that disorder generated by any lack of parallel, cylindrical molecules.

Figure 3. Two-dimensional representation of a crystal lattice.
$\underline{x}$ and $\underline{y}$ are sides of a unit cell.

The following discussion of x-ray diffraction theory is for crystals, assuming a high degree of order.

Crystals exist as a lattice of regular, three-dimensional, repeat-arrangements of ions, atoms, or molecules, the simplest (or most convenient) repeating unit being defined as the unit cell. A more rigorous definition of a crystal lattice is given in Henry, Lipson and Wooster[11] "...a regular array of points in space such that the environment of each point is exactly the same, and in the same orientation". A two dimensional representation of this concept is presented in figure (3). x and y are the axes of the unit cell. Now, it is easily seen that this regular arrangement may be represented by an infinite number of sets of parallel planes, as seen from figure (4).

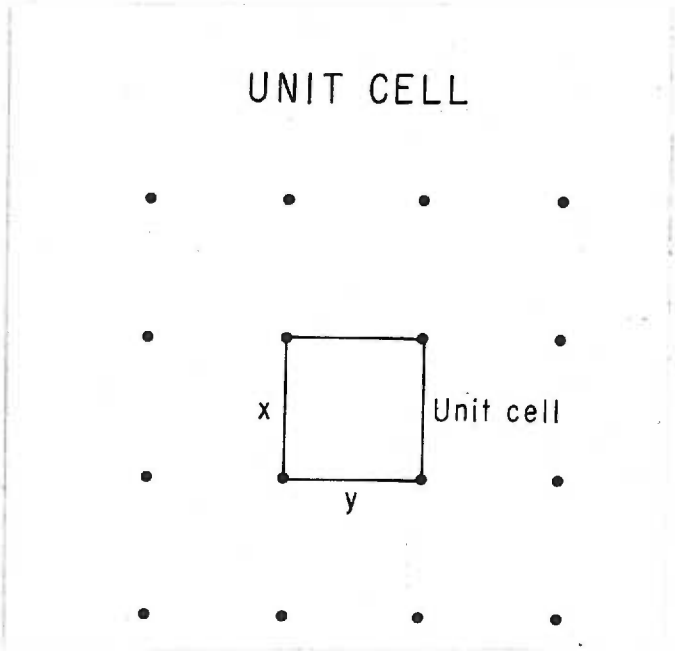

Figure 3.

Figure 4. Miller Indices (see text for description).

A useful analogy in this regard is the fruit orchard viewed while driving down a highway. As one looks at this regular arrangement of trees one notices many sets of parallel planes. A crystal is a three-dimensional fruit orchard. These planes are, by convention, named (or indexed) according to their behavior toward the unit cell. If a, b and c are the unit cell dimensions along the x, y and z axes respectively, then the planes of any particular set of planes divide these distances into $\frac{a}{h}$, $\frac{b}{k}$ and $\frac{c}{l}$, and h, k and l are called the Miller indices. Every set of planes through a unit cell has a set of indices: h denoting the number of divisions into which the planes divide the unit cell distance a (along the x-axis), k the number of divisions b is divided into (along the y-axis, l the number of divisions of c (along the z-axis).

MILLER INDICES

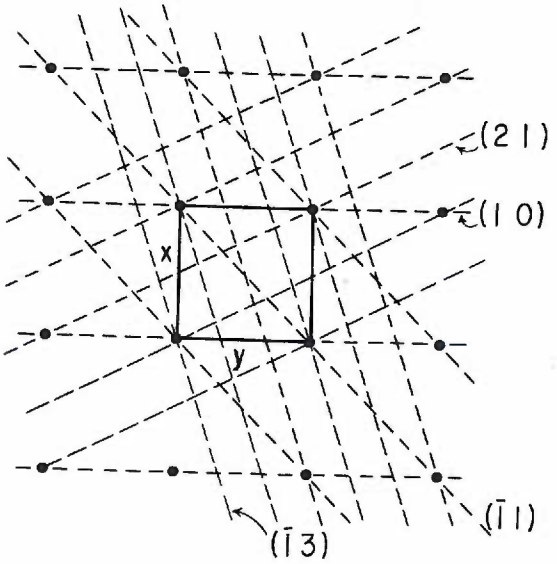

2 DIMENSIONAL LATTICE

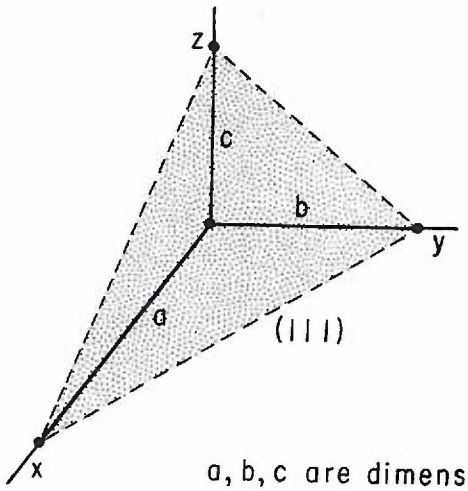

a, b, c are dimensions of a unit cell along the x, y, z axes, respectively

3 DIMENSIONAL LATTICE

By convention these h, k and l indices are always whole numbers and the notation is (hkl). In the two dimensional figure the (10) set of planes divides a (along the x-axis) into one unit, and since it is parallel to the y-axis it does not interesect this axis, and, therefore, k is zero. The (21) set of planes divides the unit cell dimension along the x-axis into two parts, that along the y-axis into one, and so on. Attention must be paid to sign; if the first plane adjacent to the origin cuts "an axis on the negative side, ...a bar is placed above the corresponding index". (Nyburg, page 24) The three-dimensional (111) planes are illustrated in the right hand part of the figure. Another identical plane is at the origin of the axes. It should be remembered that all unit cells in the crystal are cut in the same manner by each set of (hkl) planes.

X-rays are scattered by electrons of the atoms, ions and molecules comprising the crystal lattice, and for practical purposes are usually considered to be scattered from the (hkl) planes. This scattering is indicated in figure (5) by the arrows going out in random directions. In this figure at O and C are two molecules. Monochromatic, parallel incident x-rays 1 and 2 are impinging upon these two molecules which are in two adjacent planes of a set of (hkl) planes, the distance between which is d. All but a very few of the incident beams pass through the sample. Of those that are scattered, for reinforcement (diffraction) to occur there must be an integral number of wavelengths in the path difference between ray 1-1′ and ray 2-2′ (1′ and 2′ are the diffracted rays).

Now, since ACB = 1 λ, the lower wave 2-2′ travels 1 λ further

Figure 5. Bragg's Law (see text for description and proof).

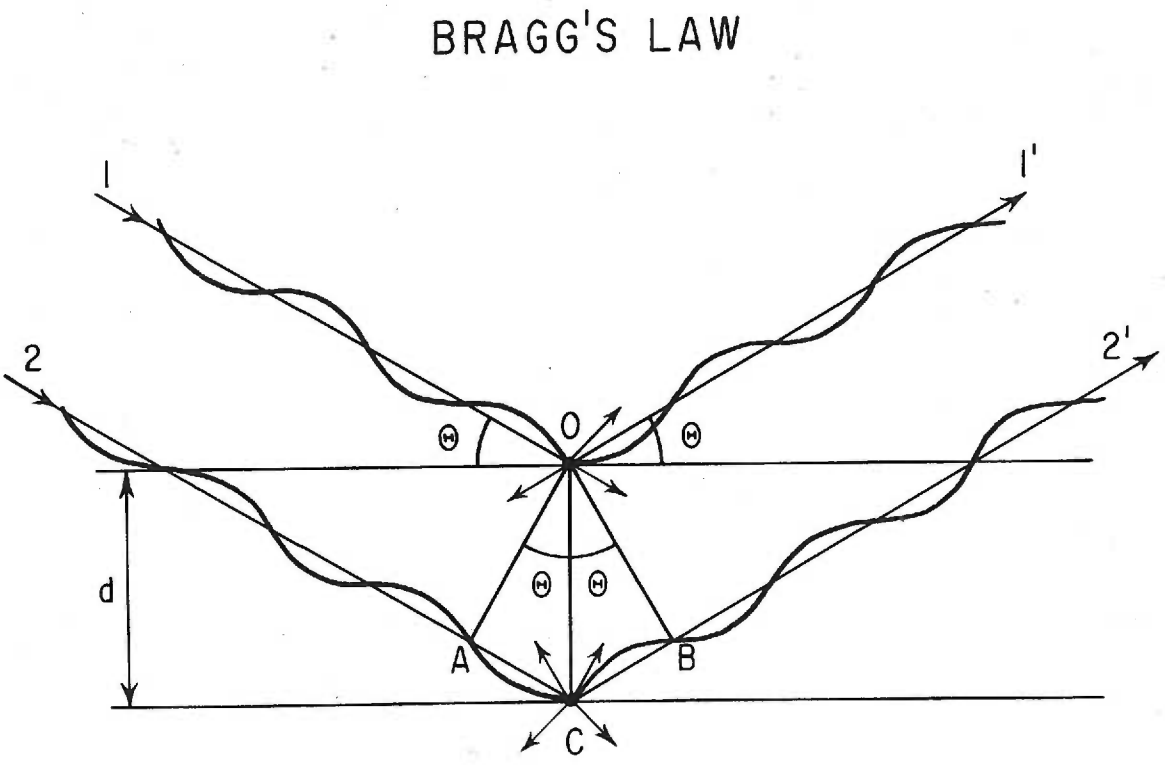

Figure 5.

than wave 1-1'. For the general case in order to have reinforcement ACB = n λ, where n is an integer. Because there are a great many parallel planes in any one set of (hkl) planes, the absolute number depending upon the size of the crystal, all scattered rays not filling exactly the above condition for reinforcement will destructively interfere. This concept is the basis of x-ray diffraction and is embodied in Bragg's Law. Mathematically this may be stated $n\lambda = 2 d \sin\theta$. The angle θ of diffraction for any set of (hkl) planes will depend upon the interplanar distance $d_{(hkl)}$. In the figure let d be the distance between any two planes of a set of parallel (hkl) planes. OA is drawn perpendicular to the incident rays 1 and 2 striking the successive planes. Angle AOC = θ, triangle CAO is a right triangle, and OC = d.

$$\text{Sin}\,\theta = \frac{AC}{OC} = \frac{AC}{d}$$

$$AC = 1/2\,\lambda, \text{ therefore}$$

$$2\,AC = \lambda, \text{ and}$$

$$\sin\theta = \frac{\lambda}{2d}; \text{ transforming,}$$

$$\lambda = 2 d \sin\theta.$$

The condition for reinforcement will recur at ACB = 2 λ, 3 λ, etc. Hence, the general equation for Bragg's Law becomes $n\lambda = 2 d \sin\theta$, n, an integer, denoting the order of diffraction. θ is called the Bragg angle. Each set of (hkl) planes has its own unique value for d.

It is seen that the sum total of diffractions at the Bragg angle for any set of (hkl) planes will diffract as a small beam since the crystal is usually on the order of 0.2 mm in thickness. This beam will produce a spot on the x-ray film.

To explain the situation of a set of (hkl) planes reflecting as a

Figure 6. Diagram illustrating proof that when the reciprocal lattice points pass through a sphere, they satisfy the Bragg equation for diffraction.

lambda = wave length of the X-rays.
d = interplanar distance for this set of (hkl) planes.

spot on the x-ray film, the concept of the reciprocal lattice is used. If from an arbitrary origin 0 a distance = $\frac{\lambda}{d(hkl)}$ is taken perpendicular to each set of (hkl) planes, it can be shown that the points so generated (for all sets of (hkl) planes) will form a lattice. Each point on the lattice represents one set of (hkl) planes. This new lattice is called the reciprocal lattice. There remains now the task of discovering under what conditions the reciprocal lattice will be projected upon the film.

For this purpose it is necessary to introduce the concept of the reflecting sphere, first used by Bernal in 1924. Quoting Henry, Lipson and Wooster[11], the reflecting sphere expresses "geometrically the condition for reflection of a single wavelength from a particular set of (hkl) planes in a given crystal".

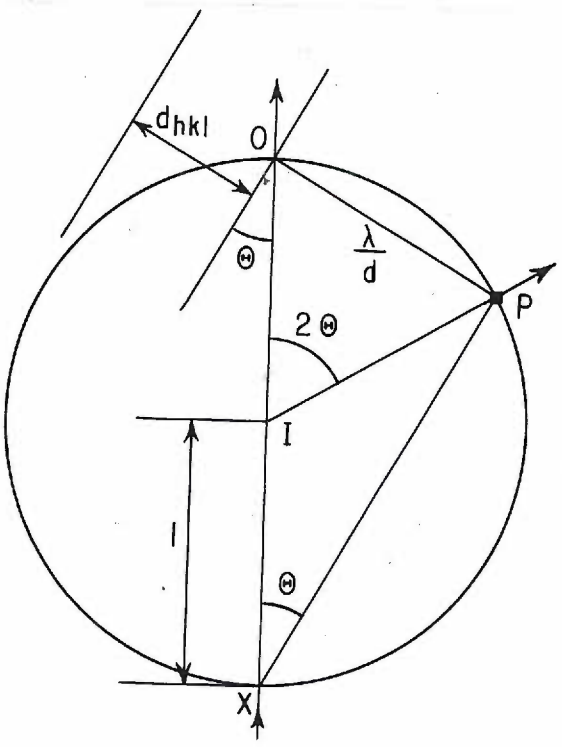

Figure 6.

In figures (7) and (8) a reciprocal lattice is constructed with the origin at 0 (in figure 8) and point (000) in figure (7). In figure (6) the orientation of the real crystal lattice with respect to the incident x-ray beam is the line XO. "At a point I , distant one unit from the origin toward the source of the x-rays, the reflecting sphere is constructed with radius one unit; this sphere passes through origin (0) of the reciprocal lattice and has as one diameter the direction of the x-rays through the origin (0)." Let P be a reciprocal lattice point lying on the sphere. It will be shown that the real lattice planes (hkl) represented by this point are in correct position relative to the incident beam for diffraction at the Bragg angle to occur. (Henry et al, page 40)

Continuing with figure (6), $d_{(hkl)}$ is, as discussed above, the interplanar distance of any set of (hkl) planes. $OP = \frac{\lambda}{d}$ is the reciprocal lattice distance and direction, by definition perpendicular to the set of (hkl) planes. Since OX is the diameter of the circle (sphere), OPX is a right triangle and $\frac{OP}{OX} = \frac{\frac{\lambda}{d}}{\frac{2}{}} = \frac{\lambda}{2d}$. Because PX is parallel to the set of (hkl) planes represented by P, angle PXO = θ .

$$\frac{OP}{OX} = \sin \theta ,$$

$$\text{therefore, } \sin \theta = \frac{\lambda}{2d}$$

$$\text{and } \lambda = 2 \, d \sin \theta .$$

Hence, the Bragg Law is satisfied, and, as shown in figures (7) and (8), the reciprocal lattice points (representing sets of (hkl) planes in the real lattice) will be in position to diffract only when they pass through the surface of the reflecting sphere. The film is, in essence, a two dimensional projection of the reciprocal lattice points, e.g. P and P′ in figure (7), on the sphere of reflection as the real and,

Figure 7. Reciprocal lattice shown rotating through the sphere of reflection. At P and P′ points on the reciprocal lattice touch the shpere of reflection, and diffraction occurs. This is indicated by the arrow from point P to the film.

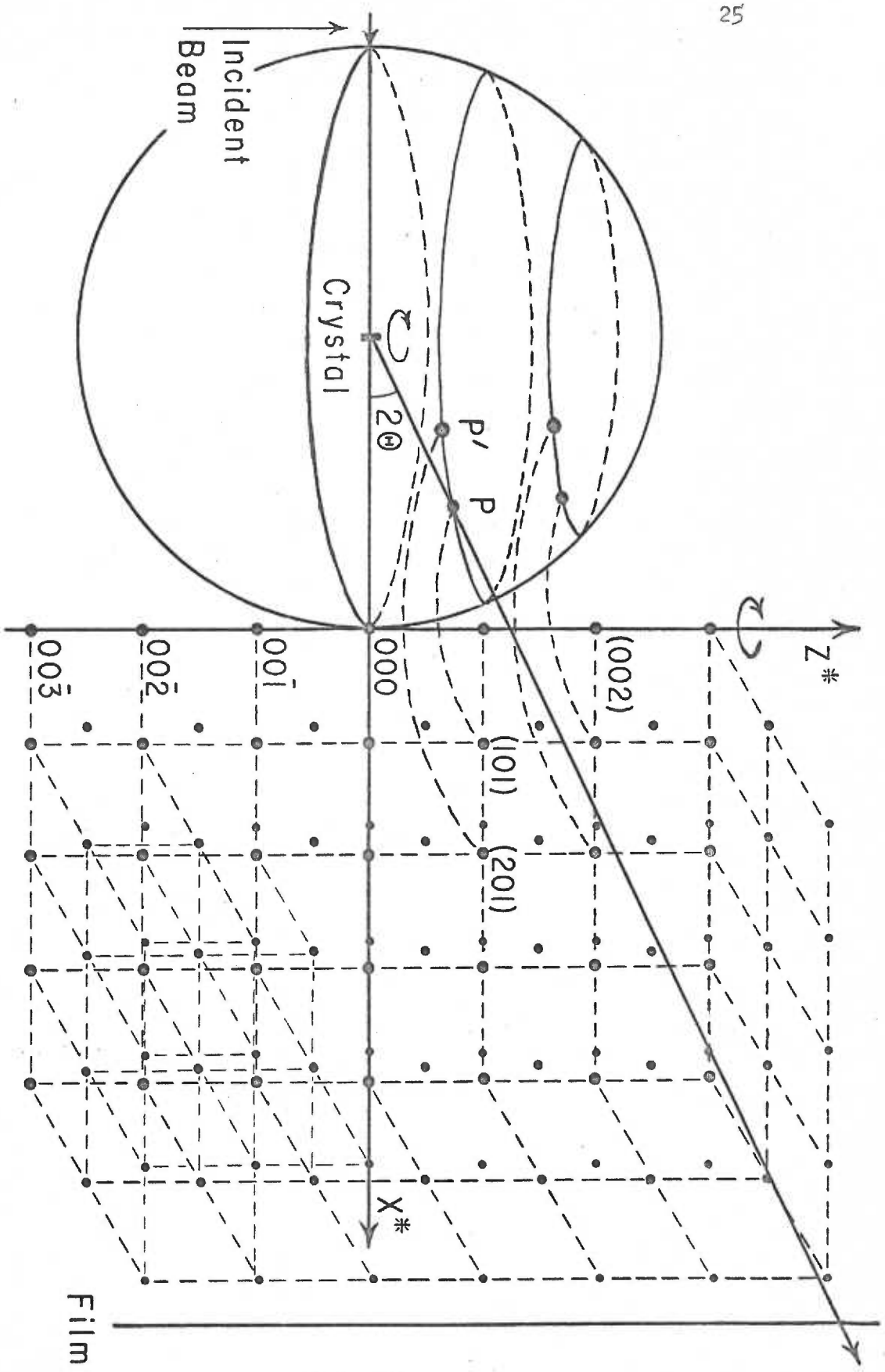

RECIPROCAL LATTICE ROTATING IN RECIPROCAL SPACE

Figure 7.

Figure 8. Diagram showing formation of row lines and layer lines.

Cylinder shows a portion of reciprocal lattice near the axis of rotation for the reciprocal lattice. All points with identical values of ξ will diffract on the same vertical row of points. All those with identical values of ζ will diffract on the same horizontal row of points (layer line).

DIAGRAM SHOWING FORMATION OF ROW LINES AND LAYER LINES

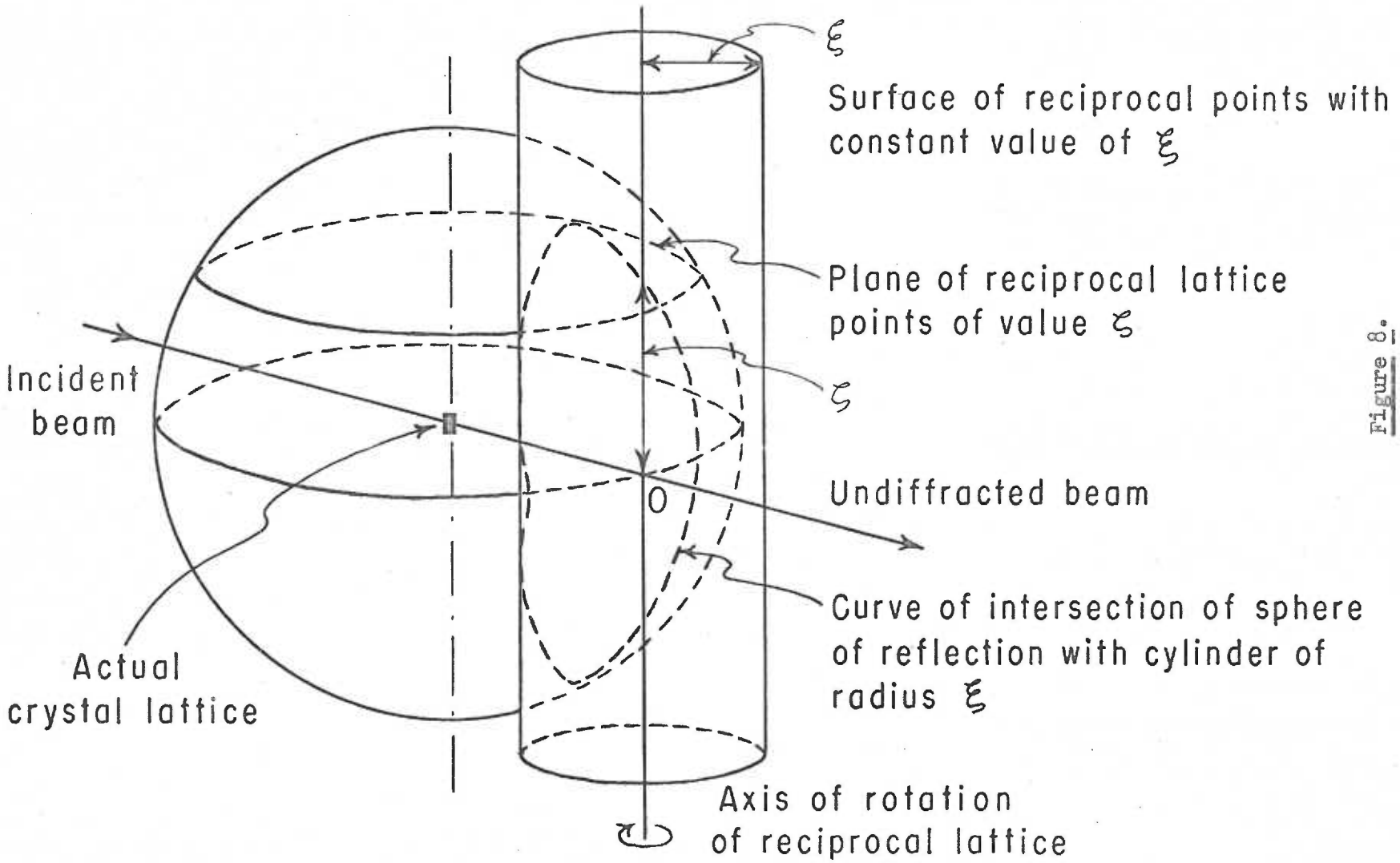

Figure 8.

consequently, the reciprocal lattice is rotated on an axis.

In figure (7), the reciprocal lattice is seen rotating through the sphere of reflection (because the crystal is rotated or oscillated through a known arc), causing the reflections to occur as the various sets of (hkl) planes come into position for diffraction. These reflections on the sphere of reflection are projected upon the film, as shown by the arrow. Since the (200) set of planes has twice the interplanar distance ($d_{(200)}$) of the (100) set and the (300) set has three times this d-value, it can be appreciated that along the reciprocal lattice axes, for example along the z* axis of the figure, the various reflecting planes of reciprocal lattice points will lie at equal intervals. The same may be said of the reflecting planes along the other two axes, a fact which necessitates a discussion of the coordinates of the reciprocal lattice.

Since the reciprocal lattice rotates through the sphere of reflection, there exists for each reciprocal lattice point three cylindrical coordinates: ζ , ξ , and Φ . The first two of these three are depicted in figure (8). ζ is the vertical distance above (or below) the origin (0) of the reciprocal lattice at which the point lies. It can readily be seen that, since the reciprocal lattice is a true lattice, there are many points with a constant value of ζ . ξ is the horizontal radius of the cylinder with an axis through the origin (0) upon which the point lies; and, as with ζ , there are potentially many points in the reciprocal lattice with the same ξ-value. Φ , which is not shown in the figure, is the angle made by a point from a plane parallel to the cylinder axis of the reciprocal lattice and perpendicular to the incident beam. Be-

cause the film is a two-dimensional projection of the reciprocal lattice points passing through the sphere of reflection, the reciprocal lattice points with the same value of ζ will reflect as horizontal lines (layer lines) on the film, and those with the same value of ξ will reflect on the same vertical line (row line). An example of this phenomenon is the diffraction pattern from the A-form of DNA. Hence, if the crystal or fiber order is of sufficient quality, the values of ζ and ξ may be obtained directly from the sharp spots on the film. This is done using a Bernal chart, which is a grid laid down over the film with values of ζ and ξ on it. Obviously, a different Bernal chart must be used for each film-specimen distance, for the distance between the same two spots will vary with film to specimen distance and the grid used for reading the reciprocal lattice coordinates will vary also.

Normally, a crystal which has $\underline{x}$, $\underline{y}$ and $\underline{z}$ axes is diffracted rotating around each axis. The successive layer lines with values ζ represent reflections from (1 kl), (2 kl), (3 kl), etc. reciprocal lattice spots when the fiber is rotated or oscillated around the x-axis; from (h 1 l), (h 2 l), (h 3 l) when rotation or oscillation is about the y-axis; and from (h k 1),(h k 2), (h k 3), etc. when rotation is about the z-axis. The row lines fill in the other two portions of the (hkl) values. It is possible to immediately find the dimensions of the unit cell of the real crystal from the layer lines, since the d-value of the first layer line directly above the origin of the film is the $d_{(100)}$, $d_{(010)}$, or $d_{(001)}$ depending upon about which axis the crystal is being rotated or oscillated. Knowing the film-specimen distance and measuring the origin to first layer line distance, the d-value may be obtained for the (100),

(010) or (001) reflections from the Bragg equation, $n\lambda = 2d\sin\theta$. $d_{(100)}$ is a, the unit cell dimension along the x-axis. Similarly, $d_{(010)}$ and $d_{(001)}$ are the unit cell dimensions b and c along the y and z-axes, respectively. Further, it can be shown that $\zeta_{001} = \frac{\lambda}{c} = \frac{\lambda}{d_{001}}$, $\zeta_{100} = \frac{\lambda}{a} = \frac{\lambda}{d_{(100)}}$, and $\zeta_{010} = \frac{\lambda}{b} = \frac{\lambda}{d_{(010)}}$.

Just as the real unit cell has three unit cell dimensions, so does the reciprocal lattice. These are noted as a*, b*, and c*. By the definition of the reciprocal lattice $a^* = \frac{\lambda}{d_{(100)}}$, $b^* = \frac{\lambda}{d_{(010)}}$, and $c^* = \frac{\lambda}{d_{(001)}}$. From these values the reciprocal lattice may be constructed if the crystal is orthogonal, as are fibers of DNA. The diffraction pattern for an orthogonal crystal is such that all four quadrants of the film are identical if the fiber or crystal is exactly perpendicular to the incident beam. Should the crystal belong to another system which has angles other than 90° between the axes, these angles would need to be known and could be measured from the film, since the (200) reflection would not lie directly above the (100).

The reciprocal lattice is constructed for each layer line, and from the values of ξ the individual reflections on the film can be indexed. The details of indexing are beyond the scope of this thesis, but an excellent discussion of the subject may be found in Henry, Lipson and Wooster[11].

In the analysis of fiber diffraction patterns, there is only one axis around which the fiber may be rotated. Due to the screw and other types of disorder in fibers of the α-helix, it is not necessary to rotate around this axis; hence, the fiber is maintained stationary, and the reciprocal lattice, rather than oscillating back and forth, in effect

rotates a full 360°. It is thus possible to measure directly only one of the unit cell dimensions - c, which is taken along the fiber axis, the z-axis. Indexing in this case becomes more ambiguous, and a trial and error method is used. The fiber axis, being the z-axis, is the vertical axis of the film. The layer lines are, therefore, h k 1, h k 2, h k 3, etc. The reflection on the zero line in the row line nearest the origin of the film is taken as the (100) reflection, the next spot on the zero layer line is taken as the (010) reflection. In case there is a reflection on a higher layer line which is closer vertically to the origin of the film than the closest reflection on the zero layer line, it is projected vertically onto the zero layer line, i.e. same row line, and this is considered to be the (100) reflection. (It should be noted that the (100) reflection may not have occurred, due to a systematic absence of this reflection.) Unless there are a good many reflections of good quality, much ambiguity in indexing will result.

Once the reflections have been indexed, in order to calculate the structure of a molecule, it is necessary to determine the intensities of the reflections. The intensity of a diffracted beam of x-rays depends upon the number of electrons diffracting in a (hkl) plane. It is proportional to the density of the reflection on the film.

The calculated intensity of diffraction from any set of (hkl) planes is given by the equation:

$$I_{(hkl)\ abs.\ calc.} = \left[\sum_r f_r \cos 2\pi (hx_r + ky_r + lz_r)\right]^2 + \left[\sum_r f_r \sin 2\pi (hx_r + ky_r + lz_r)\right]^2$$

Equation (1) (Nyburg, page 77).

Figure 9. Illustration of the concept of fractional coordinates.

Unit cell with dimensions a, b and c.

(See text for description)

Nyburg pp. 78[22]

$\sum_r$ is the sum over all the atoms of a species r, and x_r, y_r and z_r are the fractional coordinates of each atom concerned. fr is the atomic scattering factor for the atom r, e.g. a carbon atom and h, k and l are the Miller indices. The meaning of these terms will now be discussed.

A. Fractional coordinates

As a rule, the atoms of the molecules lying in any plane, and so diffracting, will not fall exactly in the plane but either below or above it. Nor do they lie exactly on the unit cell surface. If a, b,

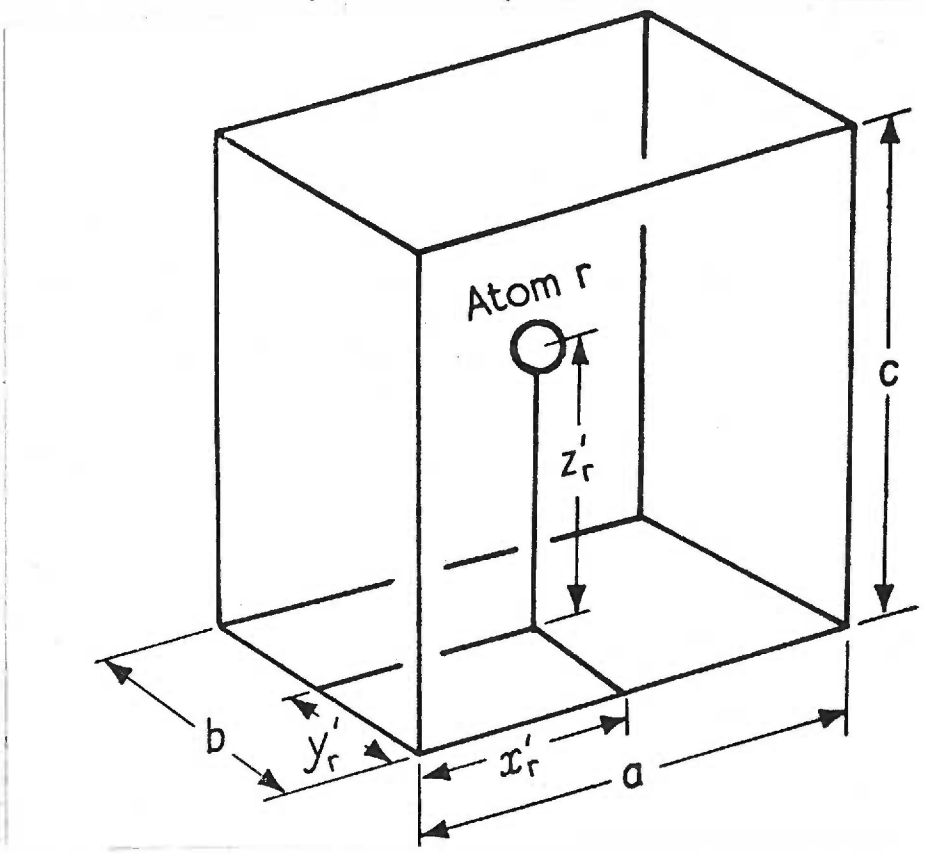

Figure 9.

Figure 10. Illustration of phase differences produced by the diffracting atoms (electrons) being out of actual (hkl) planes.

Nyburg pp. 93[22]

and c are the respective lengths of the unit cell on the x, y and z axes, respectively; if an atom (r) is somewhere within the unit cell; and if x'_r, y'_r and z'_r are actual distances of atom (r) along the three axes, then $\frac{x'_r}{a} = x_r$, $\frac{y'_r}{b} = y_r$ and $\frac{z'_r}{c} = z_r$. These values x_r, y_r and z_r are the fractional coordinates. The above relationships are illustrated in figure (9).

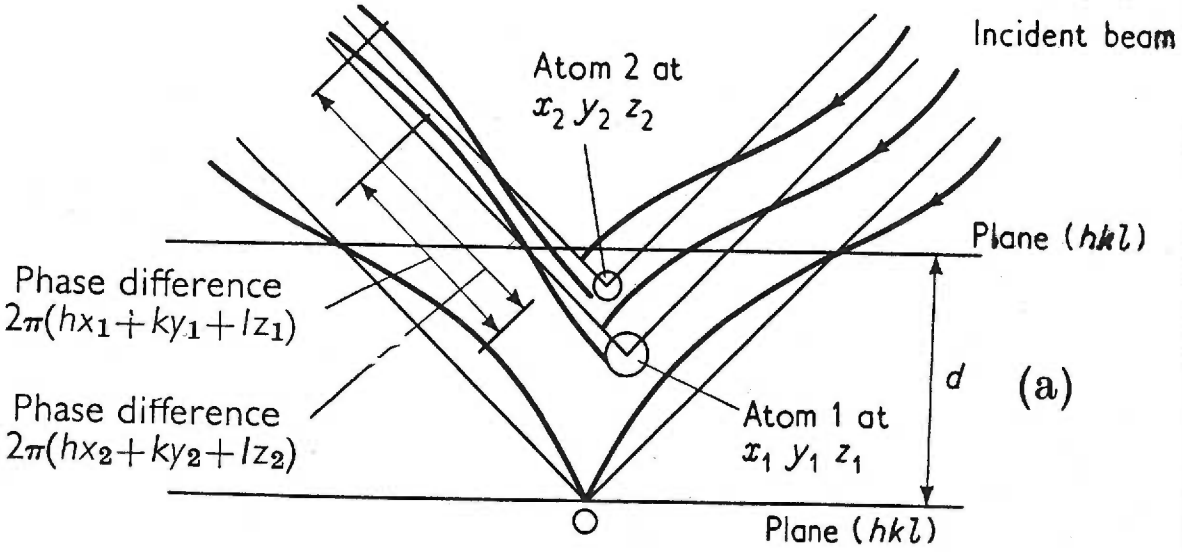

Figure 10.

The fractional coordinates are important since, by virtue of atom (r) lying outside the diffracting (hkl) planes, wave trains diffracted from atom (r) at the Bragg angle θ will be slightly out of phase with those from an atom lying in or closer to the plane. This phase difference geometrically is $2\pi(hx_r + ky_r + lz_r)$. The sum of the phase differences of waves diffracting from all the atoms (in a molecule centered in the (hkl) plane) will then act to decrease the amplitude and intensity of the diffracted wave from what it would have been if all atoms of the molecule were in the actual (hkl) plane and diffraction from these were, therefore, exactly in phase. The intensity equals the square of the amplitude so that a small change in amplitude is a larger change in intensity. (See figure 10.)

B. Atomic scattering factor (fr)

If the electrons (which, it will be remembered, are the "particles" which scatter x-rays) surrounding an atom (r) are considered a cloud of some finite volume, it may be seen that the amplitude of the wave leaving the atom will depend not only upon the number of electrons in the cloud, but also upon the direction of scattering. It can be appreciated from figure (11) (Nyburg, page 74) that x-rays scattered from two widely separated electrons in a direction parallel to the incident beam have the same amplitude as the incident ray. However, it is also clear that x-rays scattered at directions other than parallel to the incident beam will be slightly to considerably reduced in amplitude due to the destructive interference of the two rays from the two or more different electrons. Consequently, the intensities of diffracted beams at high Bragg angles θ will be considerably less than intensities of beams diffracted

Figure 11. Illustration of effect of high angle of diffraction on the intensity of diffraction. Small squares represent two diffracting electrons in the electron cloud surrounding the nucleus.

(22)
Nyburg pp. 74

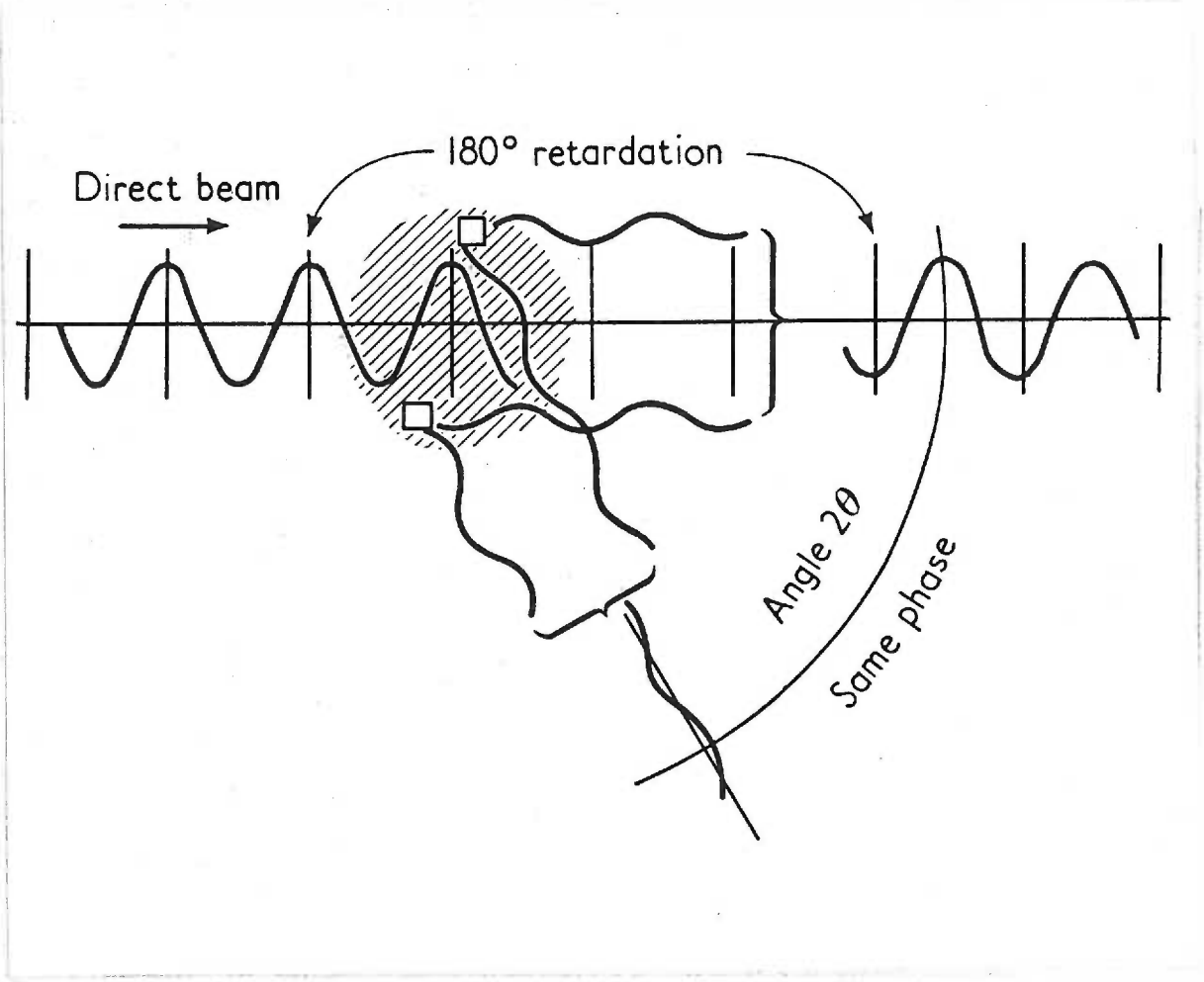

Figure 11.

at low Bragg angles. This means that the reflections on the outer portion of the film must be corrected for this decrease in intensity. Values of the scattering factor (fr) for many atoms have been tabulated at various scattering angles. The atomic scattering factor is the number of electrons (atomic number) and is considered to be in the forward direction.

In summary, the intensity of diffraction from all atoms in the molecules on the (hkl) plane is then seen to be directly proportioned to

the sum of the corrected atomic scattering factor (fr). This is modified, of course, by the phase arising from intensity differences contributed by the fact that many of the diffracting atoms do not lie in the (hkl) plane itself.

Usually, in determining molecular structures from intensity measurements, intensities themselves are not used, but rather the structure factor $F_{(hkl)}$. $[F_{(hkl)\ calc}]^2 = I_{(hkl)\ abs\ calc.}$ The structure factor $F_{(hkl)}$ is used in the Fourier transforms, which are the summations of electron densities over an infinite distance.

Any continuous, periodic function f(x) can be represented by an infinite series:

$$f(x) = a_0 + a_1, \cos x + a_2 \cos 2x + a_3 \cos 3x \cdots\cdots + b, \sin x + b_2 \sin 2x \cdots\cdots$$

Equation (2) (Nyburg, page 96).

Therefore, $f(x) = a_0 + \sum_{-\infty}^{+\infty} (a_n \cos nx + b_n \sin nx)$.

Equation (3) (Nyburg, page 96)

This summation is known as a Fourier Series. Extending the concept to a three dimensional structure which repeats (as does the unit cell in a crystal) every a, b and c along x, y and z axes, respectively, the equation becomes:

$$P(xyz) = a_{000} + \sum_{-\infty}^{+\infty} \sum_{-\infty}^{+\infty} \sum_{-\infty}^{+\infty} [a_{pqr} \cos 2\pi (px + qy + rz) + b_{pqr} \sin 2\pi (px + qy + rz)]$$

Equation (4) (Nyburg, page 98).

$\underline{p}$ is the electron density at the point xyz; xyz are fractional distances along cell edges $\underline{a}$, $\underline{b}$ and $\underline{c}$ (not to be confused with the fractional coordinates of atom $\underline{r}$ above). a_{pqr} and b_{pqr} are related to the structure factor, and, hence, equation (4) can be shown to become:

$$P(xyz)_{abs} = \frac{1}{V}\{F(000) + \sum_{-\infty}^{+\infty}\sum_{-\infty}^{+\infty}\sum_{-\infty}^{+\infty} |F(hkl)| \times \cos[2\pi(h_x+k_y+l_z) - \alpha(hkl)]\}.$$

Equation (5) (Nyburg, page 98).

$\underline{V}$ is the volume of the unit cell. $\alpha(hkl)$ is defined as "the phase by which the waves of the (hkl) reflection are ahead of those scattered at the origin of the cell". (Nyburg, page 99)

$$\tan \alpha(hkl) = \frac{\sum_{r=1}^{n} f_r \sin 2\pi(hx_r+ky_r+lz_r)}{\sum_{r=1}^{n} f_r \cos 2\pi(hx_r+ky_r+lz_r)}$$

Equation (6) (Nyburg, page 94).

Recall that the numerator and denominator of equation (6) are the same values as those presented in discussing the intensity and structure factors. Here, as before, they describe the differences in phase due to the diffracting atoms being out of the (hkl) planes. Before it is possible to calculate a three dimensional Fourier analysis, the values of the phase $\alpha(hkl)$ must be known for each structure factor. The determination of these values is beyond the scope of this discussion but may be calculated mathematically or from known atomic positions in the unit cell.

While ideally the summation of electron density should be carried out for an infinite number of terms, practically (and fortunately) the accuracy of analysis is limited by the fact that the number of visible

reflections is limited; thus, the number of structure factors is also limited. For small molecules which are highly ordered it is possible to keep the error quite small if the number of reflections for which F (hkl) has been calculated is about 1000. The electron density (p) is calculated, usually on large computers, "at all points on a suitably spaced mesh, layer by layer", (Nyburg, page 115), through the unit cell.

The above discussion deals in general terms, and is applicable to helical structures only in principle. In 1952 Cochran, Crick and Vand[8] worked out the mathematical representation of the Fourier transform for the α-helix. What follows is taken from their paper.

Any helix point is defined by the equations

$$x = r \cos (2 \pi z/P),$$

$$y = r \sin (2 \pi z/P),$$

$$z = z,$$

where r = radius and P the axial repeat spacing. These are shown in figure (12). (Cochran et al, page 582) The Fourier transform of a point in reciprocal space with reciprocal lattice coordinates ($\xi \eta \zeta$) is:

$$T(\xi \eta \zeta) = \int \exp [2 \pi i (x \xi + y \eta + z \zeta)] dV,$$

Equation (7) (Cochran et al, page 582)

dV being the volume change and proportional to dz. The transform may be simplified by the use of Bessel functions and written so that the intensity of a reflection is directly proportional to $Jn (2 \pi r R)^2$, Jn denoting the n^{th} order Bessel function (see figure (13)). (Cochran et al, page 582)

Figure 12. Real and reciprocal lattices of a continuous helis

real - left

reciprocal - right

Cochran, Crick and Vand pp. 582[8]

Figure 13. Illustration of Bessel functions

Cochran, Crick and Vand pp. 582[8]

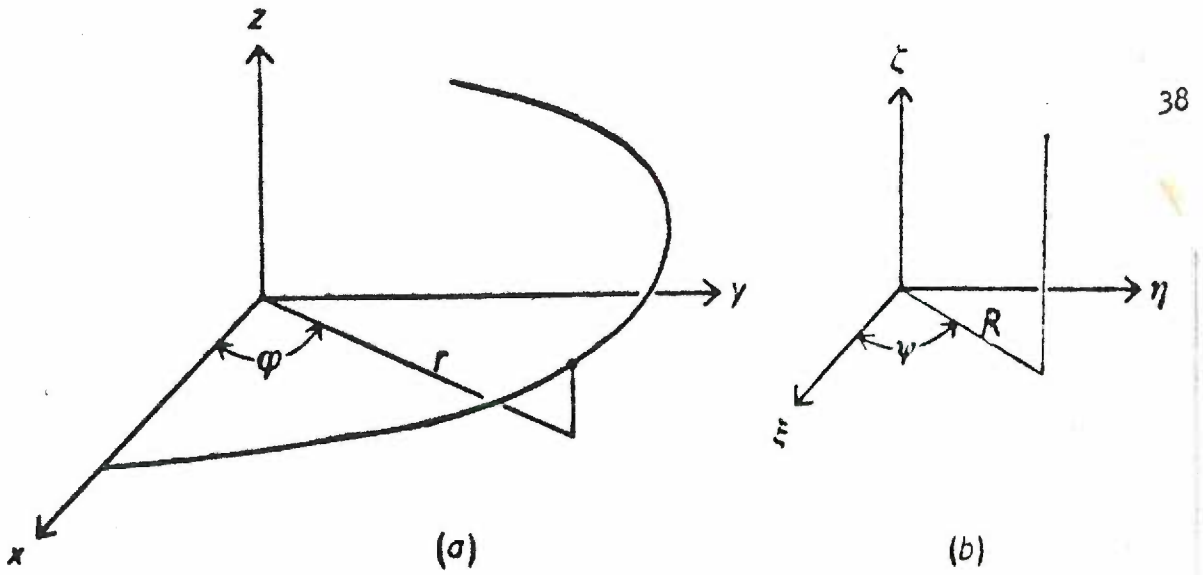

Figure 12

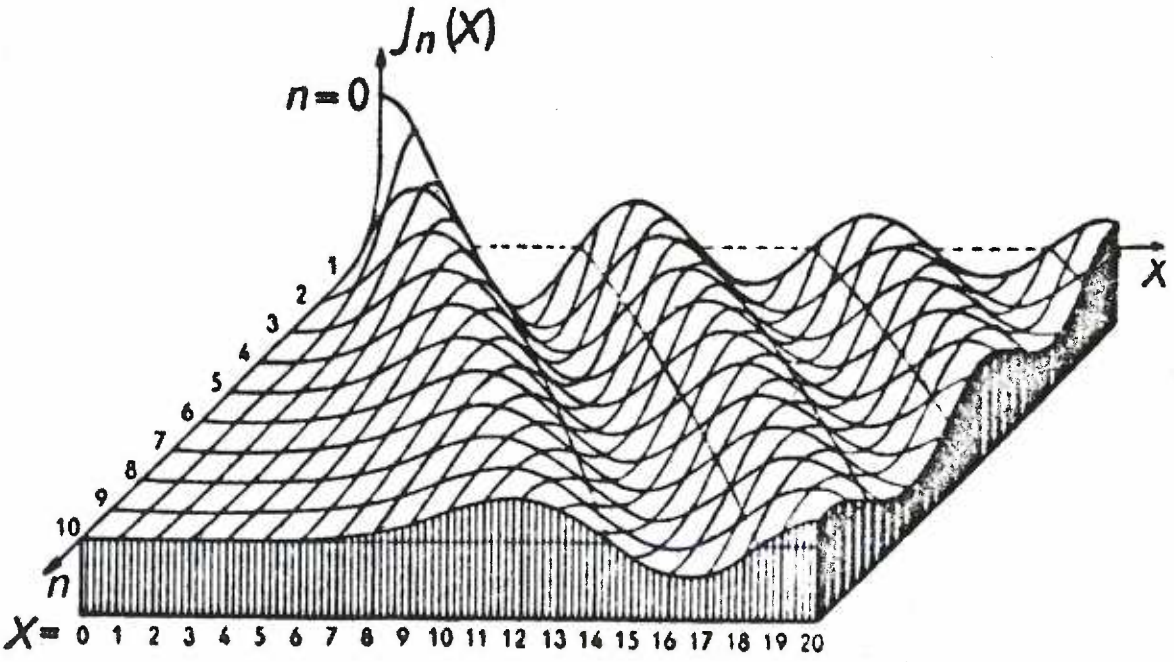

Figure 13.

R denotes the radius of the reciprocal lattice and is, therefore, $\propto \frac{1}{r}$, r the radius of the real helix. The entire Fourier transform may be written in the form $T\ (R\ \psi\ \frac{n}{P}) = Jn\ (2\ \pi\ R\ r)\ \exp\ [\ i\ n\ (\psi + 2\ \pi)]$ and gives both phase and amplitude for the n^{th} layer line. As seen from the figure depicting Bessel functions, T decreases rapidly as n increases. Now, the helix is not everywhere the same; it is a discontinuous helix, which is "a set of points with a vertical spacing P (occurring) on a continuous helix". (Cochran et al, page 583) There are only certain levels on which the above Fourier transform is finite; that is, the helix gives rise to scattering only at certain levels along its axis. These levels occur at $\zeta = \frac{n}{P} + \frac{m}{p}$, being the distance between the reciprocal lattice layers, P being the vertical repeat distance (the helix pitch) and p the vertical distance apart of the diffracting molecules on the helix. n and m are integers. As an example, DNA has a helix pitch P of 34Å and a vertical spacing (p) of the nucleotides of 3.4Å.

Upon close inspection of figure (14), a line drawing of an actual diffraction pattern from the B-form of DNA (see plate 1 for the actual photograph), it can be seen that the pattern resembles very nearly the illustration of the Bessel functions in figure (12). As the layer lines of the photograph increase (Jn increases), the intensity of reflection decreases, which in the diagram of DNA is denoted by decreasing line density. As discussed above, each (horizontal) layer line is generated by the passage of all the reflecting (hkl) points on the reciprocal lattice of a constant ζ through the sphere of reflection. Each spot in the layer line has a different ξ . As the reflections move away from

Figure 14. Line drawing of X-ray diffraction pattern from the B-form of DNA. 98% relative.

(See text for description.)

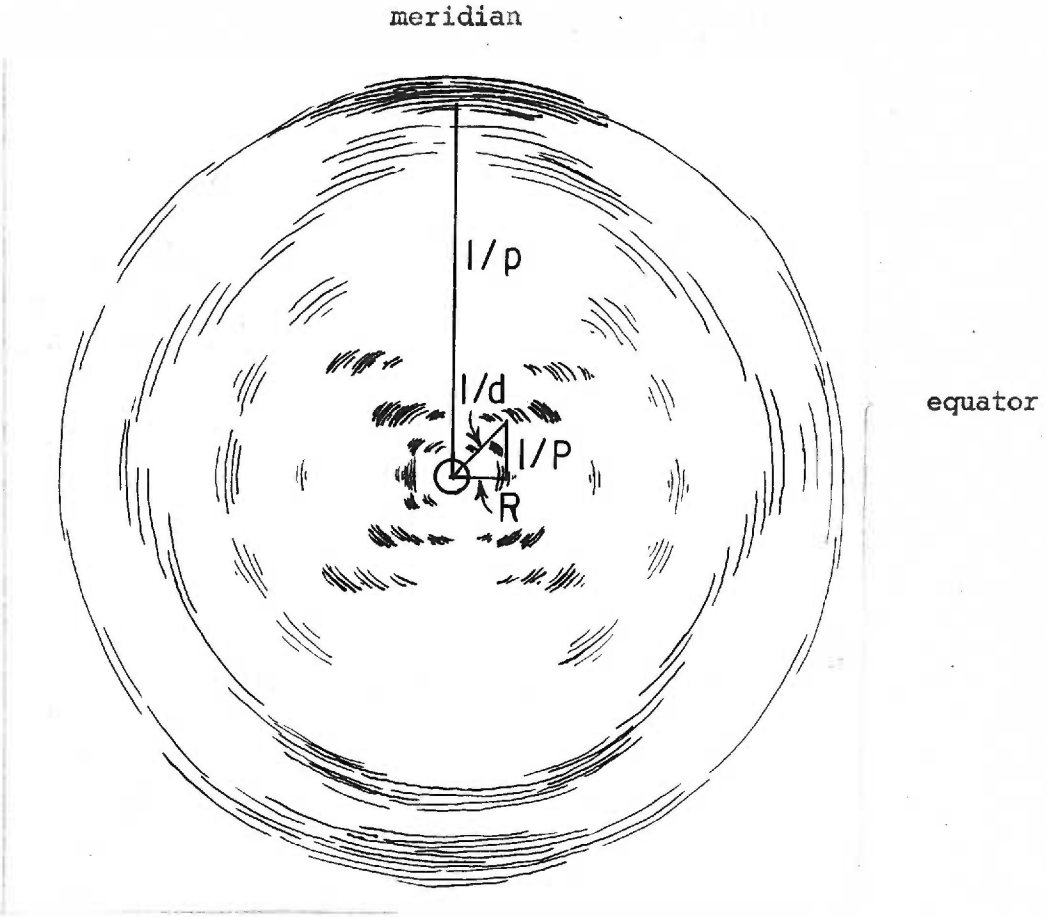

Figure 14.

the origin (center) of the film, their intensities decrease, just as do the amplitudes of the Bessel function moving out on the x-axis for a constant value of n. Furthermore, as n increases (shown on the drawing and plate 1) with increasing numbers of layer lines, the intensity decreases.

It is possible without solving the entire transform experimentally to say a great deal about the structure of α-helical substances. This is a fortunate circumstance with DNA and nucleohistone because there are few reflections and many are of poor quality (arcs or circles) making direct unambiguous solution of the transform from experimental data impossible. There are several evaluations which may be made in very little time, all of which are basic dimension of the helix: (1) whether the α-helix is present, (2) the radius of the helix, (3) the number of helically coiled strands, (4) the helix pitch P, and (5) the internucleotide (or peptide) distance. The determination of these properties is, again, based on the fact that diffraction occurs as Bessel functions with intensity (I) $\propto$ Jn $(2 \pi r R)^2$. Now, $2 \pi r R$ is the value (X) of the n^{th} order Bessel function. Therefore, by setting $X = 2 \pi r R$ it is possible to find in tables of Bessel functions the value of X and, therefore, of $2 \pi r R$ for first, second, third, etc. maxima on each layer line n. Each successive layer line is a successive value of n in the Bessel function tables. As discussed above, the atomic scattering factors are least distorted near the center of the film because the reflections here are of small Bragg angle θ. Moreover, since the reflections on the film are projections on a flat surface of those originating on a sphere, the nearer to the center of the film the more accurate will be the

measurements. Each of the above determinations will now be discussed in turn. It is important to note first that diffractions from (hkl) planes perpendicular to the fiber axis (interplanar d-values parallel to this axis) generate reflection along the meridian of the fiber, whereas reflections from (hkl) planes parallel to the fiber axis diffract along the equator of the film.

A. To determine whether or not the structure is α-helical is possible at a glance. If an α-helix is present the crossed pattern of the reflections should be present, and intensities should decrease markedly as the reflections occur further out on the film from the center.

B. The radius (r) of the helix is also easily determined because $X = 2\pi r R$. It is necessary only to determine $\underline{R}$ from the film. $\underline{R}$, as mentioned earlier, is the reciprocal lattice radius and is proportional to $\frac{1}{r}$. If $\underline{R}$ is determined from the film, which it easily can be done, the equation $X = 2\pi r R$ is solved for $\underline{r}$. $\underline{R}$ is taken along the equator of the film since, as already discussed, diffraction from sets of (hkl) planes with interplanar distances $d_{(hkl)}$ perpendicular to the helix axis (planes, themselves, parallel to the axis) diffract along the equator. This situation is readily appreciated since reciprocal lattice points of sets of (hkl) planes are taken perpendicularly to the planes of the real lattice, as defined earlier. Thus, the first reflection on the equator from the origin of the film (center of the film) is from the outside diameter of the real helix because, from consideration of the reciprocal lattice and Bragg's Law, reflections with large $d_{(hkl)}$ values have small Bragg angles ($n\lambda = 2 d \sin\theta$). As seen from the dif-

fraction photo of the B-form of DNA (plate 1) it is also the strongest, which follows from the fact that the phosphate group which has the most diffracting electrons is on the outer most part of the DNA molecule, defining the helix radius. The other (and more peripheral) equatorial reflections are due to planes parallel to the fiber (helix) axis taken through the deoxyribose and nucleotides. $\underline{R}$ is measured using the triangle shown in figure (14). The d-value of the reflection nearest the meridian is first obtained from the Bragg equation. This is seen from figure (14) and plate 1 to be directly above the very dense first zero layer line reflection from which $\underline{R}$ is determined, and the triangle with side equal to 1/d, 1/P and R is a right triangle. $\frac{1}{P}$ or $\frac{\lambda}{P}$ by definition equals $\frac{\lambda}{d_{001}}$ since it is equal to the layer line spacing which, as discussed above, equals the dimension of the unit cell around which the crystal is rotated. In the case of a fiber, the unit cell dimension which is measured is $\underline{c}$ along the z-axis. Since $\frac{1}{d}$ and $\frac{1}{P}$ are known $\underline{R}$ may be obtained by use of the Pythagorean Theorem.

C. If $\underline{r}$ is found to be about 12-14Å, there is a double stranded helix. A value of $\underline{r}$ greater than about 15Å denotes a triple stranded coil.

D. The determination of $\underline{P}$, the helix pitch, has already been discussed under the determination of $\frac{1}{P}$. Since its reflections are generated by planes along (and perpendicular to) the fiber axis, it diffracts on the meridian.

E. $\underline{p}$, the repeat distance of the nucleotides along the axis of the helix, is found by taking the d-value of the strong, diffuse meridional (10^{th} layer line) arc. Because the nucleotides are arranged in planes

along the fiber axis, they will also diffract meridionally.

Some further points will help to clarify what has been said regarding interpretation. First, the diffraction pattern actually consists of two sets of reflections: those from the large repeating distance, the helical pitch P, and those from the nucleotide repeat distance p. However, as already pointed out, the nucleotides are not homogeneous and, therefore, unlike the phosphate-deoxyribose complexes, they do not give rise to sharp reflections since the diffracting (hkl) planes are of rather poor quality. For this reason, and since the intensity of the higher order diffractions decreases rapidly as do the Bessel functions of higher n, the other layer lines from the nucleotide diffractions disappear or are very dim and diffuse. Such reflections may be seen as vague streaks coming down from the intense meridional 3.4Å ($\frac{1}{p}$) arc. When these diffuse reflections from the nucleotide (hkl) planes can be seen to occur on layer lines corresponding to those generated by the strong, more crystalline phosphate-deoxyribose complexes, then it can be said that there is an integral number of nucleotides per turn of the helix pitch. Another way of looking at this phenomenon is that when P/p is a ratio of integers, which is 10/1 for DNA, the ratio of 1/P : 1/p is also integral. Therefore, the higher order reflections from the nucleotides and the higher order reflections from the phosphate-deoxyribose groups occur on the same layer lines, and there is an integral number of nucleotides per helix pitch. Moreover, when the strong meridional reflection is established as meridional with confidence and not merely a slurring of two semi-meridional reflections due to patterns of poor quality, then the number of residues (nucleotides in DNA)

per helical turn is equal to the number of the layer line from the center of the film. Thus, in DNA the strong arc on the tenth layer line, firmly established by good diffraction patterns as being meridional, means that there are 10 nucleotides per turn of the helix. In summary, then, because (1) the layer lines of the nucleotide diffractions fall on layer lines generated by phosphate-deoxyribose groups, and (2) the diffuse, apparently meridional reflection is indeed meridional, there are <u>exactly</u> 10 nucleotides per helical turn.

It should be noted at this juncture that the author has discussed the diffraction pattern in a peculiar manner. He has not proceeded from the diffraction pattern to the model, but rather he has used the Watson-Crick model of DNA to account for the x-ray diffraction pattern. While at first glance this approach may seem retrospective, it is precisely the approach which must be taken in experimentally determined structures of very large molecules. DNA has a molecular weight of 8×10^6, nucleohistone one of about 18×10^6. To place all these atoms from a fiber diffraction pattern would not be possible. As pointed out by Wilkins,[35] it was necessary first to know the configuration of all the small groups, e.g. of the phosphate, deoxyribose and nucleotides in DNA. X-ray diffraction of <u>crystals</u> of small molecules, e.g. polynucleotides, phosphate and deoxyribose patterns, was the first step since it is possible to place the atoms if only a few are present and good crystals can be grown. From studies of these smaller molecules, which make up the macromolecules, bond angles, bond distances and three dimensional configurations of these small groups may be found. Other information from fields such as biochemistry, organic chemistry must

also be known. Only when these properties and configurations of the small groups are known is it possible to tackle the macromolecules. This is done by building models using all the known features of the small molecules and without straining known bond angles and distances. The Fourier transform is then solved for the model, and the positions and intensities of the reflections generated by the model (hkl) planes are then compared with those from the diffraction pattern. After trial and error, and repeated attempts, with varying degress of success at obtaining better oriented fibers or crystals, the model and experimental data may coincide, as it now does to a high degree of DNA.

Other classical examples of this approach to the structure of macromolecules are Perutz and Kendrew's[27] models of myoglobin and hemoglobin, Pauling and Corey's[24] discovery of the guanosine-cytosine triple hydrogen bonded configuration, Davis and Rich's[29] molecular structure of polyadenylic acid.

In view of the fact that it is necessary to have material of as high a degree of order as possible in determination of structure by x-ray diffraction, it is most convenient to have a method whereby the degree of order can be estimated. Such a tool is polarizing microscopy. Although some material, such as fibers that have too low a degree of order for good x-ray diffraction photographs, may demonstrate excellent extinction on the polarizing microscope, it is possible to determine fairly accurately the birefringence, which measures optically the degree of order present.

If a beam of plane-polarized light strikes a crystal (or an ordered fiber), it is split into two components vibrating at right angles to one another. One is called the ordinary ray and the other the extraordinary

ray. In any particular crystalline or otherwise ordered substance one or the other of these two components, traveling through the substance at right angles to one another, will be transmitted at a higher velocity than the other, i.e. the refractive indices in the two planes are different. This amount of difference is called Δn (the birefringence) and is dependent upon the degree of order in the crystal (or fiber). If there is no order the incident plane-polarized beam will not be split into the two components and $\Delta n = 0$; the material is then said to be isotropic. When order is present in a substance, the combination of ordinary and extraordinary components, viewed end-on, results in elliptically polarized light because (for each wavelength), as either ordinary or extraordinary ray is traveling faster, there is a phase difference in the two components. This phenomenon gives rise to a vibration in the plane of the analyzer of the microscope, and the crystal (or fiber) is seen as a bright entity on an otherwise darkened field. Rotation of the crystal in the beam of polarized light results in a sharp extinction, or total loss of brightness, at every 90°, for the vibration in the plane of the analyzer is lost.

The light emerging from the crystal is usually brightly colored when visualized through the analyzer, the color depending upon the physical thickness of the crystal and the birefringence, both of which determine the retardation of one of the two perpendicularly vibrating rays behind the other. The retardation is the distance (in $m\mu$) that the ordinary ray lags behind the extraordinary ray, or vice versa, assuming they both started in phase at the crystal surface.

Mathematically, the above concepts may be summed up by the equation

$\Gamma = \Delta n t$, where Γ = retardation, Δn = the birefringence and t = thickness. At certain retardation, for any wavelength λ, the two components will be $1/2\,\lambda$ out of phase, and, since the source of the plane polarized light is white (daylight), various colors will emerge. It is, therefore, possible, using a compensator or the Newton Scale of Interference Colors for Daylight, to determine experimentally the retardation, and hence the birefringence (Δn) by solving the equation $\Gamma = \Delta n t$ for Δn.

A compensator is a quartz wedge for which the retardation varies along its distance due to variation in thickness of the wedge. At any distance the retardation is known. The compensator is inserted into the microscope between the crystal and analyzer such that if the crystal has a retardation of the ordinary ray behind the extraordinary ray, the compensation has just the opposite. It is then moved along its length until it extinguishes the color emitted from the crystal, and the retardation of the crystal is thereby known from that of the compensator. The Newton Color scale is a chart of colors seen when polarizer and analyzer are crossed and parallel. For each retardation a specific pair of colors is emitted, e.g. for $\Gamma = 1376$ mμ, the color seen with the crossed polarizer and analyzer is brilliant green, that seen when they are parallel is violet.

Only those fibers with the highest Δn achievable are chosen for x-ray diffraction studies.

For the interested reader, an excellent review by H. Stanley Bennett[2] of polarizing microscopy may be found in McClung's Handbook of Microscopical Techniques.

A word should be said in closing the introduction about fibers.

They are not crystals, for in a crystal there is the same degree of order throughout. In a fiber, however, there are areas of fairly good order interspersed with areas ranging from poor order to tangled and coiled helices. Diffraction proceeds from the most ordered parts of the fiber, and background scattering of x-rays from the unordered parts. The ratio of ordered to unordered substance in the fiber depends, as noted earlier, upon the purity of the substance and how much stress has been placed upon the gel - how much stress birefringence has been induced. What intrinsic birefringence is present is dependent upon the homogeneity and purity of the material.

MATERIALS AND METHODS

A. Extraction and Purification

Calf thymus was chosen as the source of the deoxyribonucleohistone due to its high content of this substance and its availability. Calf thymus was obtained from Swift and Co. packing plant from calves which had been slaughtered only 10 minutes previously. The organs were immediately placed in liquid N_2 for fast freezing to prevent the enzymatic destruction of the deoxyribonucleohistone. Thereafter, the thymi are stored at -59° C until used.

The nucleohistone was extracted by the general method of Zubay and Doty.[40] This method was used because of the ease of obtaining good quantities of nucleohistone on repeated extractions. Extraction and purification was carried out at about 4-6° C.

Five grams of fresh frozen calf thymus is homogenized in 50 ml. of a solution 0.075 M in Li Cl and 0.024 M in Li EDTA (ethylenediaminetetraacetic acid) adjusted to pH = 8. Nucleohistone is least soluble in 0.1 M solutions while almost all other proteins are soluble at this concentration, and pH= 8 is the isoelectric point for the nucleohistone. Lithium salts are used throughout the extraction and purification procedures instead of sodium salts because of the low molecular weight of Li as compared to Na and its consequent lesser influence on the intensities of the x-ray diffraction spots. To the original homogenization solution is added 0.25 ml. of caprylic alcohol, which together with the EDTA, according to Zubay and Doty, inactivate the DNA arc. Homogenization is done in the Vir-Tis instrument at 60 volts for 1 minute and 30 volts for 4 minutes. The homogenate is then strained through 4 layers

of bolting cloth, which has been washed with glass distilled water, and then is centrifuged at 400 xg for 10 minutes. The supernatant is decanted; and the sediment, containing the deoxyribonucleohistone, is dispersed in 50 ml. of 0.075 M Li Cl - 0.024 M Li EDTA solution of pH = 8, to which is added 0.12 ml. caprylic alcohol. Dispersion is accomplished by homogenizing for 5 seconds at 60 volts and 30 seconds at 20 volts, Centrifugation of this suspension is then carried out at 400 xg for 10 minutes. The washing process is repeated a total of six times. The final sediment, containing almost entirely deoxyribonucleohistone along with some fibrous proteins and cell debris not filtered out with the bolting cloth, is suspended in 0.0002 M lithium phosphate solution adjusted to pH = 6.8 by rapid (60 volt) dispersion with the homogenizer for 20 seconds. This suspension is then quickly transferred to a 600 ml. beaker, the total volume of solution brought up to 200 ml. by the addition of more 0.0002 M lithium phosphate solution. It is stirred rapidly for 1 hour by a Mag Mix stirrer and achieves a very good suspension in this time. Too little solution leads to too great a dispersion; too great a volume leads to aggregation. Glass distilled water of fluorometer reading 24 ppm is used throughout the extraction and purification procedures.

The suspension is now brought up to 0.1 M salt concentration by the addition of 200 ml. of 0.2 M Li Cl after centrifuging at 400 xg to remove cell debris. Deoxyribonucleohistone precipitates from solution as a white floc and is centrifuged from the Li Cl at 400 xg x 20 minutes. This sediment is again suspended in about 150 ml. of 0.0002 M. lithium phosphate solution pH = 6.8 by homogenizing first for 10 seconds and

then stirring rapidly for 1 hour with the Mag Mix. The final suspension is purified by dialysis of approximately 100 ml. of suspension against 5 liters of 0.0002 M lithium phosphate solution pH 6.8 for 2 weeks, the lithium phosphate solution being changed 3-4 times during dialysis. Following dialysis the deoxyribonucleohistone solution is stored at 4° C until drawn into fibers. Ultraviolet spectrographic analysis is carried out using a Beckman DB Spectrophotometer to determine the approximate concentration of nuclechistone.

B. Drawing out of fibers

About 10 cc of the purified deoxyribonucleohistone suspension is centrifuged at 10,000 xg for 1/2 hour to remove any aggregation which may have formed during storage. The pellet is discarded and the supernatant is decanted into a clean 5 cc polyethylene centrifuge tube and spun at 134,200 xg for 2 hours in the Spinco Model L Preparatory Ultracentrifuge using the SW 39 head. Ultracentrifugation results in a small amount, (about 100 mg), or viscous gel after the supernatant is decanted.

A small amount, approximately 0.05 ml., is pipetted into the jaws of a vise-like fiber stretcher (see diagram next page). This drop of viscous suspension, suspended between the two jaws, is allowed to dry at cool room temperature while keeping it as cylindrical as possible. The drying process is followed under the dissecting microscope. As it begins to reach the solid state, usually first at one end of the viscous cylinder, the jaws of the "fiber stretcher" are gradually separated resulting in a fiber about five to six times as long as the original viscous cylinder. This stretching process results in greater orientation

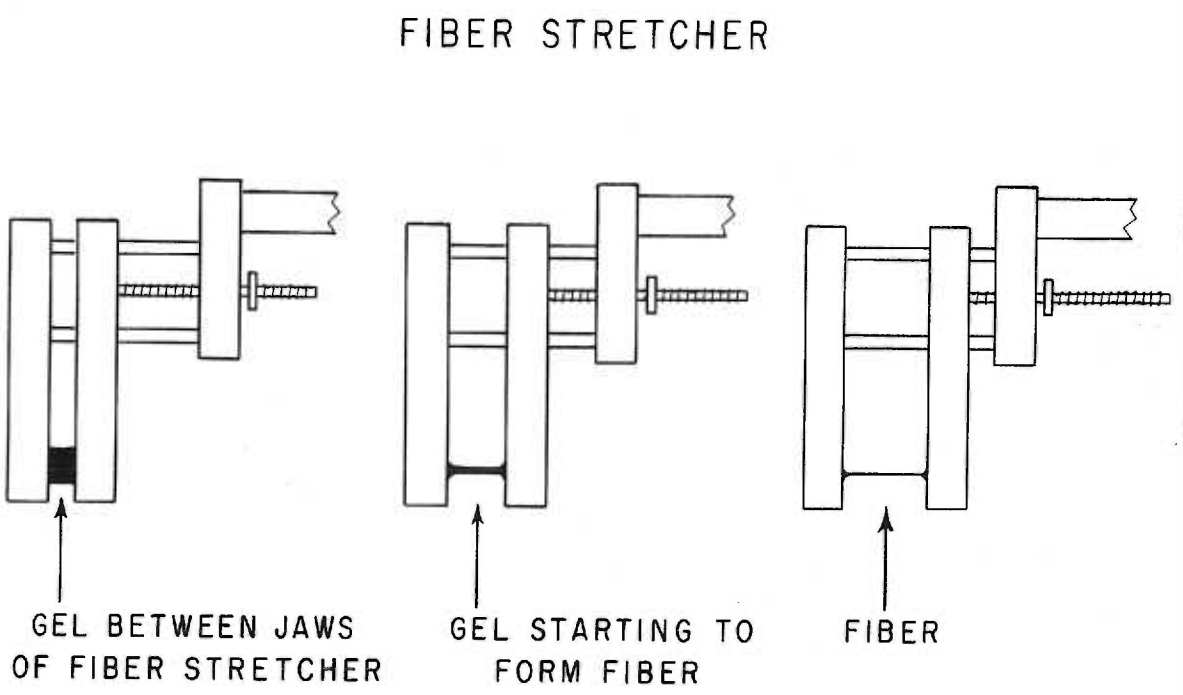

Figure 15

in the fibers with their axes oriented along the fiber length.

The partially dried fiber then is examined under the polarizing microscope, and those fibers with high order negative birefringence are chosen for diffraction. Best results are obtained when the drying suspension has been kept a good cylinder and stretching has been slow.

C. Obtaining the x-ray diffraction photographs

Selected fibers are mounted for diffraction in a Norelco X-Ray Diffraction Microcamera, which has been modified by the insertion of a

sleeve between the fiber-holder and the film to increase the specimen (fiber) to film distance, thereby allowing the low angle (high d-value) reflections to be recorded on the film.

The fiber holder itself is made from galvanized aluminum in the shape of a "U" on one side of which has been glued a strip of thin spring metal, attached at one end only, as illustrated. The other end

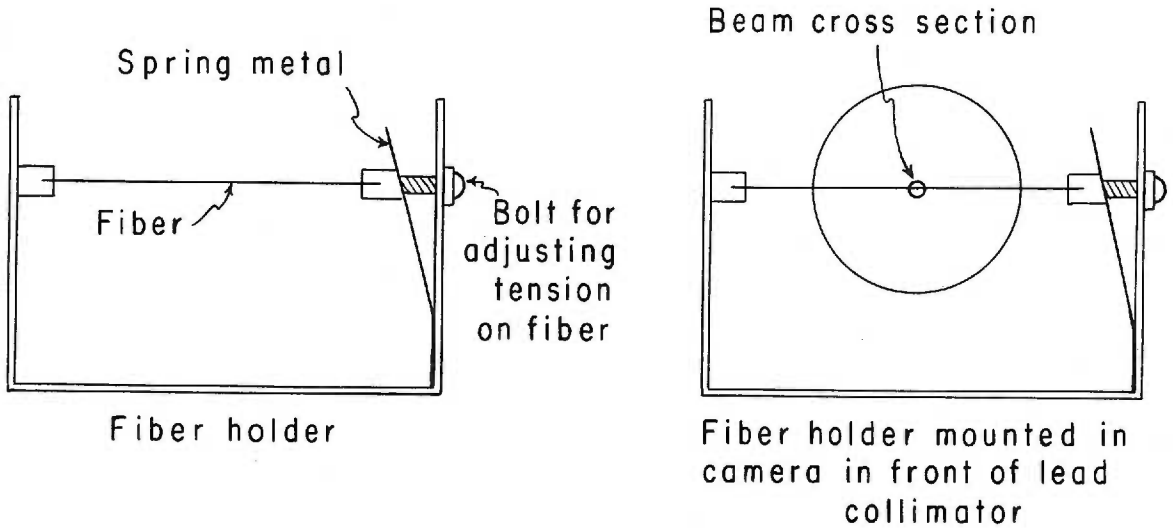

Figure 16

is held away from the frame of the fiber-holder with a small bolt. By turning the bolt the fiber, glued with Duco cement across the fiber-holder (see illustration), may be kept under a small amount of tension,

thus increasing the order in the fiber by the addition of more strain birefringence.

After the Duco cement holding the fiber in place has dried, the fiber-holder is mounted in the half of the camera containing the collimator. It is aligned optically by placing the camera on a microscope stage and shining the lamp through the collimator. The fiber-holder is then adjusted so that the fiber is in the center of the collimated beam of light. The film (Eastman Kodak No Screen Medical X-ray Film or Ilford No Screen X-ray Film) is cut to the size of the film-holder in the dark room, a hole punched in its center for the x-ray beam to pass through, the film-holder mounted in the camera, which is then assembled and placed on the track of the x-ray diffraction machine. This machine was built by Dr. Lyle Jensen at the University of Washington Medical School, Department of Anatomy, and employs a GE Ca -7 x-ray tube, with a copper target emitting a characteristic λ of 1.54 $^{\circ}$ A.

Next the microcamera is aligned with the x-ray beam by passing the x-ray beam through the collimator, through the hole in the film-holder to a fluorescent beam stop covered with lead glass. The camera is adjusted until the maximum intensity of the beam is reached.

Since air diffracts x-rays and the exposure times are relatively long, it is desirable to take the pictures in a helium atmosphere. Also, best fiber order is obtained at a very high relative humidity. Therefore, helium is bubbled through a saturated solution of $Pb(NO_3)_2$ giving a helium atmosphere of 98% relative humidity, or through a saturated solution of sodium tartrate which gives a relative humidity of 92%.

The diagram (figure 17) on the following page illustrates these relations. Film to specimen distances were at 12 mm, 30 mm and 60 mm to obtain virtually the entire diffraction pattern.

After an exposure varying between 35 and 75 hours, depending upon the film-specimen distance, the films were removed from the camera (two films, one in front of the other, were used to minimize the effects of any overexposure), and developed for 5 minutes in Kodak D-19 Developer. Than, after passing through an acetic acid bath, they were fixed for 10 minutes, rinsed for one half hour and dried at room temperature.

When dry, the films were placed on a view box and the positions on the spots were measured with a vernier millimeter scale to the nearest 1/50 mm. Because of the center hole in the film (for passage of the transmitted beam) it was not possible to find the exact center of the film; but, since the four quadrants of fiber photographs are virtually identical, the distance between the corresponding spots (or arcs) was measured and divided by two. The obvious 3.4Å meridional arc was chosen as a standard to determine accurately the film-specimen distance. Knowing both the film-specimen distance and the distance of the reflection from the center of the film, the Bragg angle may be determined trigonometrically, and from this the Bragg equation, $n\lambda = 2d \sin\theta$, is solved for $d_{(hkl)}$ values for each reflection. P, p and r may thus be obtained.

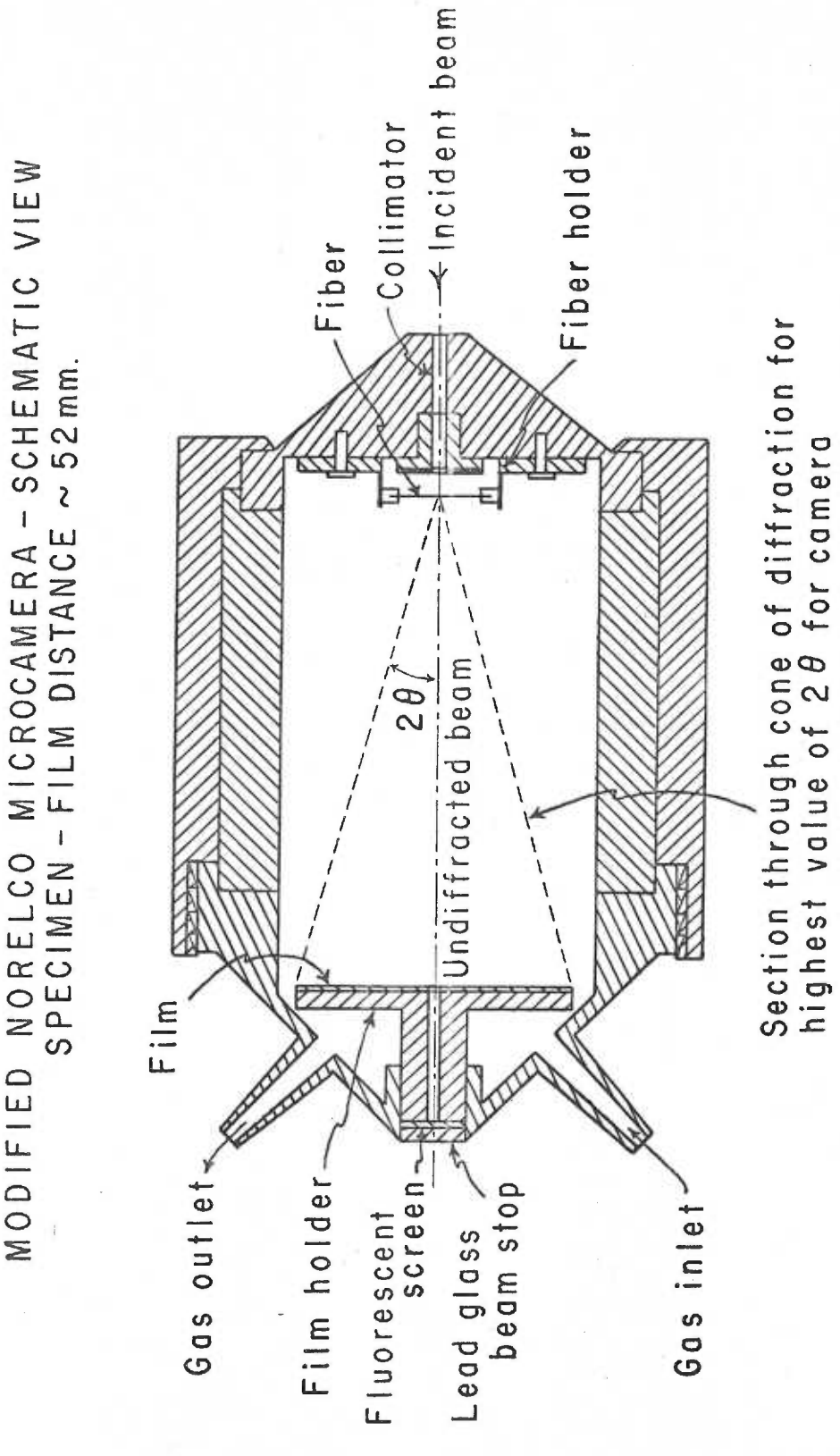
MODIFIED NORELCO MICROCAMERA - SCHEMATIC VIEW
SPECIMEN - FILM DISTANCE ~ 52 mm.
Fiber
Collimator
Incident beam
Fiber holder
2θ
Undiffracted beam
Section through cone of diffraction for highest value of 2θ for camera
Film
Gas outlet
Film holder
Fluorescent screen
Lead glass beam stop
Gas inlet

Figure 17.

RESULTS

A. Extraction and Purification of the Nucleohistone.

The Zubay and Doty[40] extraction worked very well, each extraction giving sufficient DNH for pulling about two dozen fibers, provided the entire suspension was used within a few weeks of the end of the two week dialysis period. The reason for allowing a few weeks only before the suspension was considered "old" is based upon Zubay and Wilkins[41] finding that histone would undergo denaturation to the beta-configuration after several weeks storage.

After dialyzing, the suspension was analyzed on the Beckman DB Spectrophotometer, as noted in the section on Materials and Methods. This analysis gave consistently reproducible results with high dilutions (1:25) of the DNH suspension. There were always a maximum at 260 mu and a minimum at 237 to 238 mu in the ultraviolet range.

About sixty fibers were pulled in nine months time, and of these only about six demonstrated high enough birefringence for good diffraction.

B. The Diffraction Patterns.

Two films, one of excellent quality, were obtained from the same position on one fiber. The first film (Film #2) of DNH, taken with an exposure of 35 hours at 92% relative humidity, shows well the DNA phosphate-deoxyribose backbone, which diffracts as a cross-shaped pattern in the center of the film. It also shows clearly the meridional 3.4 Å arc from the nucleotides, the inter-nucleotide distance. There are equatorial reflections at 22.8 Å and 13.3 Å, the former representing the diameter of the DNA molecule. A diffuse ring

occurs at about 10 Å and a poorly oriented, probably helical pattern at 4.5 Å. This latter reflection has a measurement along a direction parallel to the meridian of about 5.8 Å. One of these 4.5 Å reflections is seen in each of the quadrants of the film, as are the much sharper reflections from the DNA helix. These arc-like reflections do not have a d-value characteristic of any B-form DNA value.

There is also a faint 3.0 Å arc on the meridian which is not seen in the DNA diffraction pattern, but one similar to it is noted in the crystalline A-form and the crystalline lithium salt of the B-form. However, this film gives evidence of much less order than either of those two forms. Probably, then, this 3.0 A arc is not from the DNA component of the fiber.

The second DNH film (Film #3) is taken at a specimen-film distance of 61.6 mm., and is underexposed. Nevertheless, it shows the 22.8 Å equatorial reflection and a strong, sharp 47.3 Å equatorial reflection. The intense halo around the perforation in the film is probably an artifact and is generated by a small amount of the transmitted x-ray beam hitting the film. No other reflections could be noted on this film.

As a control and comparison for the DNH diffraction patterns, the pattern for the B-form of DNA was obtained using highly purified DNA given the author by Dr. D. R. Davies at the National Institutes of Health. This material, originally from Worthington Biological Supply, gave excellent sodium-DNA patterns at 98% relative humidity. To demonstrate the effect of changing water concentration, the fiber was dehydrated from 98% to 86% relative humidity, and the A-form was obtained, which shows the layer and row lines characteristic of highly crystalline materials.

FILM # 1

DNA at 98% relative humidity, specimen - film distance = 28.1 mm.

Scale 1.5/1

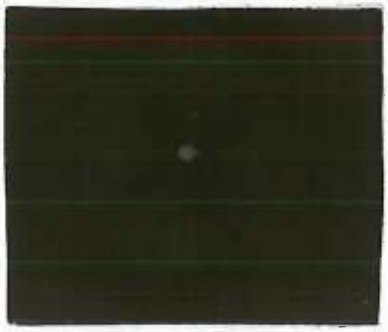

equator

meridian
B-form DNA

The intense reflections in the center of the film which form a cross pattern are from the first 5 orders (n) of diffraction from the phosphate - deoxyribose backbone of the DNA helix. The reflection for n = 4 is missing, a systematic absence. The high intensity of this set of reflections is due to the fact that phosphorus has many diffracting electrons and contributes the most to the intensity. The nucleotide purine and pyrimidine bases generate the intense arcs on the meridian. The first equatorial reflection defines the diameter of the helix. On the film this is the R measurement. The other helical reflections from the bases are seen as diffuse streaks toward the periphery if the pattern. The other equatorial reflections are generated by other planes through the fiber which are parallel to the fiber axis.

Scale 1.5/1

equator

meridian
A-form DNA
86% relative humidity

Compare this crystalline pattern to the semi-crystalline one of the B-form. Note the well defined layer lines and row lines. This crystalline pattern results from dehydration of the molecule and its consequent more compact form.

PLATE 1

Film #1 — Exposure time: 7 hr.

DNA B-form, fiber — Voltage: 40 KV

Δn= high order white — Amperage 20 ma

Relative humidity: 98%

Specimen - film distance: 28.1 mm.

Reflection	-	+	h mm	tan 2θ	2θ	θ	sin θ	2 sin θ	d (Å)
Meridional arc $\frac{1}{P}$	89.08	116.70	13.81	.49160	26°11'	13°6'	.22647	.45294	3.4
Meridional meas. 1st Layer Line $\frac{1}{P}$	101.24	103.76	1.26	.04486	2°35'	1°18'	.02257	.04514	34.1
Meridional meas. 2nd Layer Line	99.98	104.90	2.46	.08829	5°3'	2°31'	.04402	.08804	17.5
Meridional meas. 3rd Layer Line	98.68	106.14	3.73	.13279	7°34'	3°47'	.06592	.13184	11.6
Meridional meas. 4th Layer Line		This reflection is missing-systematic absence.							
Meridional meas. 5th Layer Line	95.88	108.80	6.46	.22997	12°57'	6°29'	.11280	.22560	6.8
Backbone defining helix #1	69.04	73.34	2.15	.07654	4°23'	2°11'	.03819	.06538	20.2
Backbone defining helix #2	67.50	74.86	3.68	.13101	7°29'	3°44'	.06523	.13046	11.8
Backbone defining helix #3	65.88	77.54	5.83	.20755	11°44'	5°52'	.10215	.20430	7.5
Backbone defining helix #4		This reflection is missing-systematic absence.							
Backbone defining helix #5	63.26	79.16	7.95	.28302	15°48'	7°54'	.13747	.27494	5.6
Equatorial Reflections									
#1 (nearest center) $\frac{R}{}$	85.28	89.08	1.90	.06764	3°52'	1°56'	.03377	.06754	228
#2	82.24	92.00	4.88	.17372	9°51'	4°56'	.08588	.17176	9.0
#3	79.16	95.16	8.00	.28480	15°54'	7°57'	.13828	.27656	5.6

TABLE 1

FILM # 2

DNH at 92% relative humidity,

film - specimen distance = 12.9 mm.

1.	Faint Meridional Arc	3.0 Å
2.	Meridional Arc	3.4 Å
3.	Diffuse Helical Arcs	4.5 Å
	Meridional dimension	5.8 Å
4.	Sharp Helical Spots	12.2 Å
	Meridional dimension	18.1 Å
5.	Diffuse Ring	10.2 Å
6.	Equatorial spot nearest center	22.7 Å
7.	Outer Equatorial Spot	13.3 Å

meridian

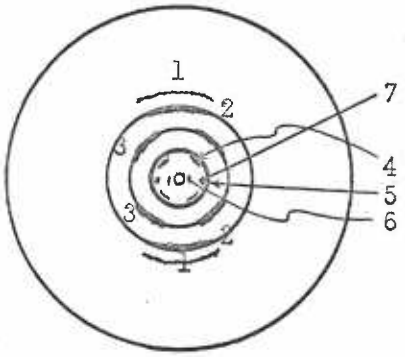

Schematic Diagram of Film #2

meridian

equator

Scale 1.5/1

(hold film up to light)

Film # 2

PLATE 2

Film #2 Exposure time: 35 Hr.

DNH fiber

$\Delta n = 0.015$

Relative humidity: 92% Specimen-film distance: 12.9 mm.

Reflection	-	+	h mm	tan 2θ	2θ	θ	sinθ	2 sinθ	d Å
Meridional arc $\frac{1}{p}$	66.22	79.00	6.35	.49163	26°11'	13°5'	.22647	.45294	3.4
Faint Meridional arc	65.20	80.02	7.35	.56452	29°27'	14°43'	.25415	.50830	3.0
Meridional meas. 1st Layer Line	71.24	73.44	1.10	.08514	4°52'	2°26'	.04246	.08492	18.1
Meridional meas. for diffuse set of 4 reflections (helix)	Meridional distance between 2 7.0		3.50	.27090	15°10'	7°35'	.13220	.26440	5.8
Spots defining helix (sharp)	66.58	69.90	1.66	.12750	7°16'	3°38'	.06337	.12674	12.2
Diffuse spots defining helix	63.68	72.76	4.54	.35140	19°22'	9°41'	.16817	.33634	4.5
Diffuse circle peripheral to sharp helical spots	Distance across diameter 3.90		1.95	.15093	8°35'	4°18'	.07483	.14966	10.2
Equatorial spot nearest center	Film ctr. 59.92	60.80	0.88	.06759	3°52'	1°56'	.03374	.06748	22.7
Outer equatorial reflection	58.50	61.45	1.50	.11610	6°37'	3°19'	.05773	.11546	13.3

TABLE 2

FILM # 3

DNH at 92% relative humidity

film - specimen distance = 61.6 mm.

1. Inner Equatorial Spot 47.3 Å
2. Outer Equatorial Spot 22.8 Å

equator

meridian

meridian

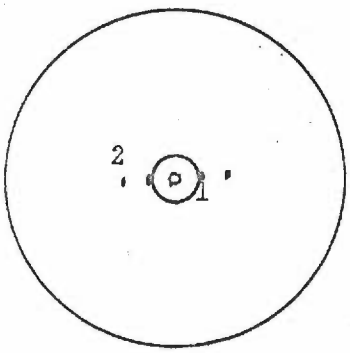

Upper film lay in front of and in contact with lower film. Lower film shows inner equatorial reflection better than upper film since the halo (artifact) does not partially overlie this reflection in the lower film.

Meridional spot probably artifact.

(hold films up to light)

Scale 1.5/1

equator

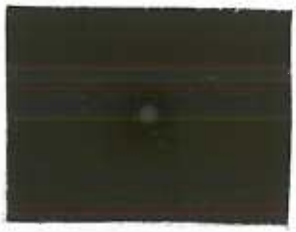

meridian

PLATE 3

Film #3 — Exposure time: 75 Hr.

DNH fiber — Voltage: 40 KV

Δn: 0.015 — Amperage 17 ma

Relative humidity: 92%

Specimen - film distance: 61.6 mm.

Reflection	-	+	h mm	tan 2θ	2θ	θ	sinθ	2 sinθ	d Å
Inner Equatorial	72.22	76.20	1.99	.03249	1°58'	0°56'	.01626	.03252	47.3
Outer Equatorial	70.12	78.5	4.20	.06823	3°54'	1°57'	.3377	.06754	22.8

TABLE 3

DISCUSSION

It is appropriate first to discuss briefly the fibers on which the studies were carried out. DNH proved to be much more difficult to work with than those of DNA. The reason for this was the aggregation of the DNH gel into virtually one large mass after centrifugation for ninety minutes. This phenomenon, certainly expected because of the property of the arginine-rich fraction to aggregate, led to much difficulty in maintaining the cylindrical form of the gel while drawing it into a fiber. Even when this difficulty could be overcome (a rare occasion), the aggregates frequently prevented good birefringence. Nevertheless, the best fiber showed sufficient birefringence for diffraction, and it is from this fiber that the significant results were obtained. It had a birefringence of about .015, which proved good enough to give an oriented diffraction pattern.

Both DNA and DNH fibers exhibited an interesting phenomenon when breathed lightly upon or when equilibrated at a relative humidity above 92%. They increased their length by about 20% in the case of DNA and up to about 100% in the case of DNH. In the latter instance, this was accomplished with very little decrease in thickness, indicating an open structure into which the water molecules could readily penetrate. As the fibers became hydrated, their birefringence increased considerably, a fact which accounted for Wilkins and Zubay[38] obtaining oriented pattern only at very high relative humidity. Water would pass in and out very rapidly enabling one to watch under the polarizing microscope a decrease in birefringence to about 0.1 of the original birefringence in less than a minute. Water, therefore, must be an important part of

the structure. Wilkins and Zubay[38] found that, at 92% relative humidity, their fibers contained 30% water, while at 75% relative humidity they contained only 17%. At 66% relative humidity the author could find only a widened 3.4Å arc as evidence of order. The remainder of the pattern consisted of diffuse circles.

With DNA, at a glance it can easily be seen how great an effect the water concentration has. The B-form is diffracted at 98% relative humidity, the crystalline A-form at 86%. Both patterns were obtained from the same portion of the same fiber of sodium DNA.

The significance of the effect of water concentration on three dimensional configuration of both DNA and DNH will be discussed later.

The films obtained by the author resemble quite closely in their general outline those reported by Wilkins and Zubay in 1959[38]. It must be noted, however, that at this writing the author has obtained only a portion of the complete pattern, that is only the part of the pattern which can be seen at a film-specimen distance of about 13 mm. This includes reflections from 3.00Å to 22.8Å. The author has diffracted at a film-specimen distance of 60 mm the same fiber for which the above values were obtained, and has found an additional equatorial reflection at 47Å. The film, however, was considerably underexposed. At the present time, Drs. Catherine Skinner and V. Sasisekharan in Dr. D. R. Davies laboratory at the National Institutes of Health are diffracting these fibers at other film-specimen distances. The author is, therefore, able to discuss only those values occurring between 3.00Å and 22.7Å, and also the 47.3 Å reflection.

There are certain differences between the author's films and those

obtained by Wilkins and Zubay[38]. This situation probably arises because of the fact that the films described here are somewhat sharper than those of the other two authors. First, however, the similarities should be noted and explained.

By reference to plate 2, it may be seen that there are definite similarities to DNA. There is the striking 3.4Å meridional reflection, which, it will be noted, is about as well ordered as that reflection of the DNA; also the 22.7Å equatorial reflection of the DNH compares in shaprness and intensity to the 22.8Å reflection of the DNA. (This is the reflection on the equator nearest the perforation in the film, only one of which is visible in the DNH film since this film, fortunately, was slightly off center.) The 34Å set of reflections of the DNH film (found on the first layer line as the part of the cross closest to the center) is not represented on either of the author's films, because, again, it was not possible to record reflections with d-values this high at a film-specimen distance of 13 mm. This reflection is seen, however, on Wilkins and Zubay's film. The second-order reflection (n=2 in the Bragg equation) from the phosphorous-deoxyribose backbone is, however, present on the author's as well as Wilkins and Zubay's[38] film. The set of (hkl) planes responsible for these phosphate-deoxyribose backbone reflections of orders n=1, 2, 3 and 5, gives rise to this second order set of four spots, one in each quadrant of the film, and has a d-value of 12.2Å on the DNH and 11.8Å on the DNA film. Because these reflections are not from crystalline DNA and are, consequently, somewhat diffuse, they agree in position and, approximately, in intensity. Measured parallel to the fiber axis (toward the meridian), they re-

present second order reflections of P, the helix pitch.

The interpretation, then, of this much of the author's (and Wilkins and Zubay's[38]) film is that the above reflections represent well oriented DNA in the Watson-Crick configuration with the long axis of the α-helix of DNA parallel to the fiber axis. The 3.4Å reflection is the inter-nucleotide repeat distance along the helix axis, the 22.8Å reflection = 2 r, the diameter of the DNA helix. The strong reflections forming the cross, measuring 18.1Å and 17.5Å meridionally on the DNH and DNA respectively represent, as just noted, the helix pitch of DNA, the difference in the two values residing in the inaccuracy of measurement of the DNH values.

The differences between the author's pattern and that of Wilkins and Zubay[38], arising most likely from better resolution in the author's films, are as follows:

(1) there is another reflection at 4.5-4.6Å which is definitely broken up into four sectors, similar to the central cross defining the helix pitch; it measures meridionally about 5.8Å, which is only an estimate since the four sectors are diffuse and difficult to measure accurately;

(2) there is a diffuse 10-12Å ring of moderate intensity upon which is superimposed a 13.3Å equatorial reflection;

(3) there is an intense 47Å equatorial reflection which is very sharp;

(4) there is a faint, but sharp, 3.00Å meridional arc on the author's film, not seen on that of Wilkins and Zubay.

It takes careful scrutiny of the film to see some of these reflections,

but they are, nonetheless, present and must be accounted for. Each will be discussed in order.

1. The 4.5-4.6Å reflections which are broken up into four sectors. The most obvious conclusion regarding these reflections is that they are part of the DNA pattern. There are simply streaks in this area on the Wilkins-Zubay film which they attribute to DNA. These streaks are part of the poorly ordered Bessel function pattern from the nucleotides of DNA in the DNA films (B-form). Since there are definitely four sectors, it might be thought that they are higher order reflections from the phosphate-deoxyribose backbone. This hypothesis cannot be entirely ruled out, particularly since they appear to lie on an extension of the same cross as the DNA components. However, the d-value (4.5-4.6Å) and the meridional measurement (about 5.8Å) do not compare with any of those seen on the DNA film, e.g. for the fifth order (fifth layer line) reflections from the DNA phosphate-deoxyribose backbone; the values are d = 5.6Å, meridional measurement = 6.8Å. This outer cross also appears considerably less well oriented than the inner, a condition not seen with DNA. For these reasons, it seems possible that this cross may be a reflection from the histone. Histones were thought by Zubay and Wilkins[41] to exist mainly in the α-helical configuration. They, however, found that at higher relative humidity the histone pattern of DNH disappeared, and their diffuse 4.5Å reflection was from the lumps of histone and dry DNH reconstituted from DNA and histone.

Pauling and Corey[23] state that from their models, the pitch of the α-helix for proteins is 5.44A. In discussing the pattern of poly-γ-benzyl-L-glutamate these authors[25] state that the c-axis trans-

lation (measurement along the meridian) is 5.76Å, which would correspond rather well with the 5.8Å off meridional reflection which the author has obtained. 5.8Å, it should be remembered, is only an estimate because of lack of sharpness of this reflection. The diffuseness of these arcs is also interesting because it indicates a rather poorly oriented set of (hkl) planes, a phenomenon which might be expected from the stresses put upon the histone α-helix by virtue of its being bound to DNA by whatever means. It, moreover, might be expected that the arginine-rich fraction would contribute most importantly to this disorder since arginine-rich histones are most strongly bound to DNA, as noted in Phillips' review[28].

(2) That there is a diffuse 10-13Å ring upon which is superimposed a 13.3Å (approximately) equatorial spot is of interest. This equatorial reflection does not appear on Wilkins and Zubay's film and possibly is related to the appearance of the 4.5Å set of arcs just discussed. If so, this might well represent the diameter of a single α-helix from the histone. Pauling and Corey[23] note that the α-keratin helix has a diameter of about 10A, including side chains. The diameter would be increased somewhat by histone side chain - DNA linkages. Also, interactions between adjacent side chains and steric hindrance to α-helix formation by proline, as pointed out by Pauling and Corey[23] and Bernal[3], could lead to compound helix formation, giving a helix diameter of about 13Å (Pauling and Corey[23]). The author has obtained no strong meridional diffraction in the region of 60-70Å which would be expected if compound helix formation occurred. In the author's camera, 60A diffraction is not visible because of scattering of the transmitted

beam (see plates 4 and 5) giving rise to a halo on the film around the perforation which is where the 60-70Å reflections would be reflected.

Zubay and Wilkins in discussing their dry histone patterns noted a 10A diffuse ring seen in α-helices.

(3) At 47Å there is a sharp, very intense equatorial reflection. This reflection was also not reported by Wilkins and Zubay[38]. Were the histone α-helix more or less oriented along and roughly parallel to the DNA α-helix, and were there two strands of histone between two DNA helices, then the diameters of two histone helices plus the diameter of one DNA helix would add up to about 47Å, and this 47Å reflection would occur on the equator (see figure (14)).

That it is possible that the histones are aligned parallel to the DNA in an α-helical manner comes from the discussion of the first two points. In the first place, should the poorly oriented, but nevertheless present, set of four reflections (forming the outer cross at d = 4.5Å) represent the α-helical histone pattern, then they must lie along the axis of the fiber and be parallel to the better ordered DNA helices. Secondly, the 12.8Å equatorial reflection would require it to be so oriented since equatorial reflections are diffracted from planes parallel to the fiber axis.

A rather serious limitation to fitting the histone into an α-helix is the lack of a meridional reflection, similar to the 3.4Å reflection, at 1.5Å. Perutz[27] points out that the 1.5Å reflection is exhibited by the α-helix alone of all helices and is, therefore, of great diagnostic value. The reason for its absence is unaccounted for by the author's explanations above. Possible reasons are:

(a) that it would lie at the periphery of the film (but still able to be seen) and would be, as a result, of too low intensity to see at this time of exposure;

(b) that there is insufficient order in the histone to reflect;

(c) that it is a systematic absence in DNH fibers.

(4) There is, however, a very faint but sharp meridional reflection at 3.0Å, which could, of course, be from sets of (hkl) planes occurring at intervals of twice the inter-amino acid residue distance along the α -helix. Such a reflection could occur from side chains which repeat every second turn of the α-helix. Pauling and Corey[25] state such a situation is found in clam muscle and porcupine quill.

It would also be possible to account for this meridional 3.0 Å reflection in another way. Hair and muscle may be reversibly stretched to about 100% elongation[25] and would, then, have a helix pitch of about 3.0Å. Since nucleohistone gels are stretched considerably upon drying, such might be the case here. It would be most likely to occur in the very-lysine rich fraction, which, due to the steric hindrance to α -helix formation by the high (9-14 mole %) proline content, could exist in the β-configuration even prior to stretching. The very-lysine rich fraction contributes about 20% to the total histone, and a faint meridional reflection from this β-configuration would be expected to occur. Were this 3.0Å meridional reflection from a β-helix the helix would be parallel to that of the DNA.

Although the above ideas are speculations from interpretations of the x-ray diffraction patterns, so are those of Wilkins, Zubay, Luzzati and Nicolaieff. It is difficult to accept the ideas of these

authors that the DNA is merely set in an unoriented gel of histone. If this situation were to exist it would be hard to imagine how the differences in the ability of the lysine-rich and arginine-rich fractions to supress RNA synthesis could occur(14). It would also be difficult to account for about 20% of the DNA being uncomplexed with histone(5). It would further be difficult to imagine any order in gene expression, which order obviously exists. Finally, how would DNA replicate if it were smothered in a gel of histone?

A very tentative model is presented which would seem to account for the interpretation of the x-ray diffraction pattern as an ordered structure of DNA with histone molecules filling in the interstices between the parallel DNA molecules, and running parallel to them (figure (18)). This model is an idealized one because the x-ray diffraction patterns do not support anything that is this well ordered. It leaves plenty of room for molecules to enter the helices. There would be numerous breaks in the histone along its axis. The suggested model would account nicely for the remarkable stretching of the fiber seen on hydration. The loose bonding of the histone to the DNA would allow the gliding of the histone along the DNA helix, and this process would be repeated throughout the fiber width.

As to the mode of attachment of histone to DNA, this may well be by salt bridges. Kirby(17) believes that the divalent cations such as calcium and magnesium may accomplish the bonding. It must be a loose bonding, able to break apart at high water concentration, such as ionic bonding through divalent cations would provide. The x-ray diffraction studies presented do not elucidate the nature of the bonds themselves.

The variation in the water content might, as Luzzati and Nicolaieff(20)

Figure 18

DNH - Tentative Model for ordered portion of fiber with 30% water concentration.

Scale 11.4 Å = 1 cm.

Small open circles are the histone helices.
Histone planes generate equatorial 13.3 Å reflection.

Large dotted circles are the DNA helices.
Diameter of DNA helices generates 22.8 Å reflection.

Cross-hatched hexagonal areas represent possible DNH unit.
This unit represents the 47.3 Å reflection. Calculated, this unit should reflect about 46.6 Å. Agreement is, therefore, within less than 1 Å.

All of these reflections, being from diameters of units which are parallel to the fiber axis, would be expected to generate <u>equatorial</u> reflections.

(Compare with Figure 1.)

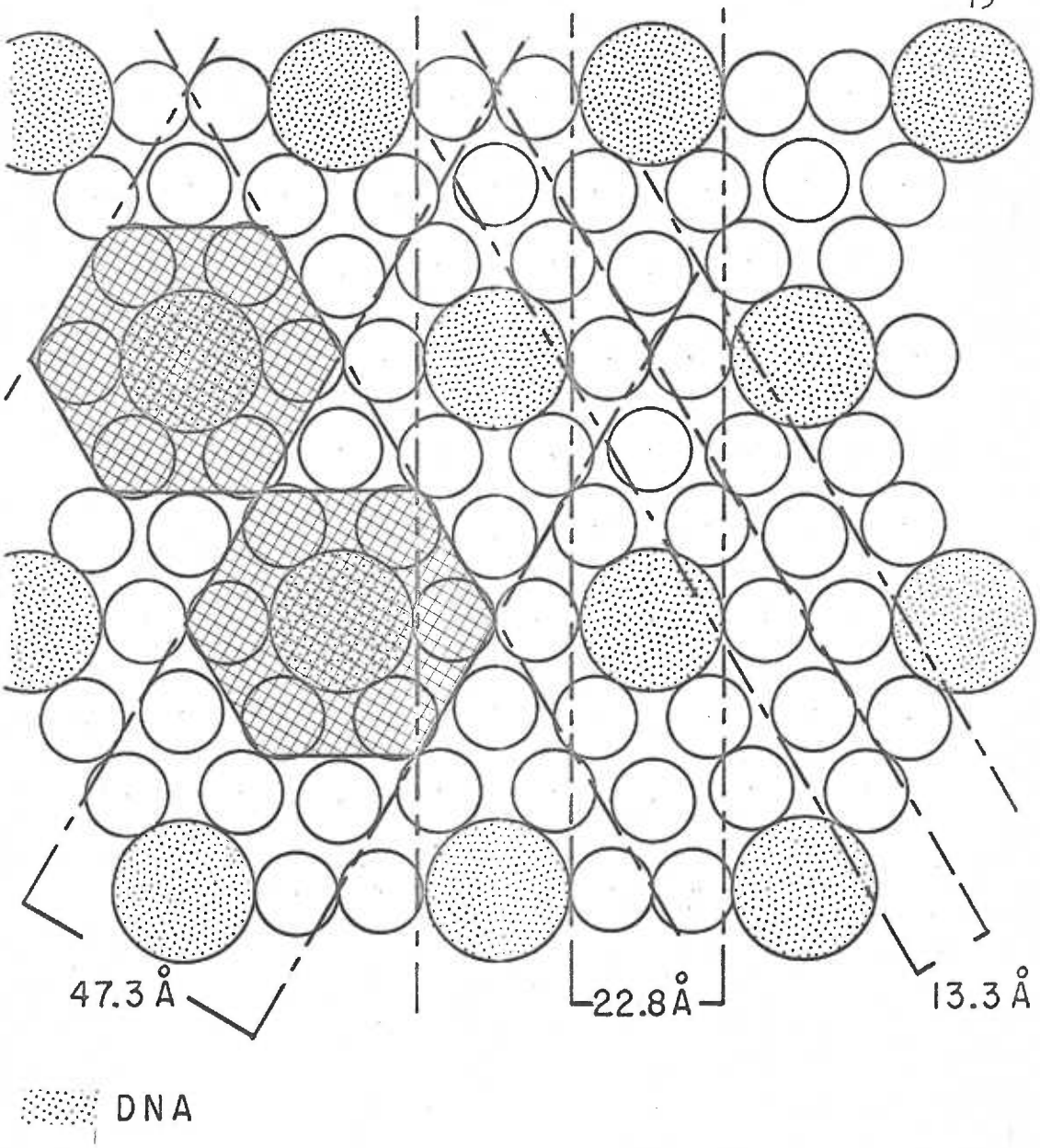

DNH - Tentative Model for ordered portion of fiber with 30% water concentration.

Figure 18

note, determine the structure of DNH at any moment and may determine the type and amount of histone bonded to the DNA, consequently contributing to the amount of DNA available for RNA synthesis. For example, it would not be inconceivable that some of the more lysine-rich histones, in bonding less strongly than the arginine-rich fractions, would become unbound to the DNA with only slight increase in water concentration, or may move to more stable positions on the DNA helix. The evidence for water affecting structure has already been presented and is dealt with, as noted in the Introduction to this thesis, by Zubay and Wilkins(41).

There are further experiments which could be done to answer some of the questions raised by this discussion. First among them is an attempt, as is now being carried out, to obtain the entire diffraction pattern of DNH. It would also be of considerable interest to fractionate native histone, draw fibers and see if by x-ray diffraction the α-helix exists for them at high relative humidity. This would help to decide whether or not histone exists natively in the α-helical configuration in DNH. Models should be built when all of this various information is available, and the Fourier Transforms of these models should be compared with an accurate determination of the intensities as well as the positions of the reflections in the x-ray diffraction pattern.

It has not proved possible to index the reflections unambiguously, since all of the data are not available, and consequently, not much would have been gained by attempting the indexing. After obtaining the entire pattern, this step should be carried out in order to obtain the Miller indices for the (hkl) planes which are necessary in solving

SUMMARY AND CONCLUSIONS

X-ray diffraction studies have been carried out on fibers of calf thymus nucleohistone prepared by the method of Zubay and Doty[40], slightly modified by the author. This study was made in order to ellucidate, if possible, the relationship of histone molecule to the DNA.

A well oriented fiber gave a semicrystalline pattern at high (92%) relative humidity indicating that the DNA is well oriented with the parallel to the fiber axis, and in this respect, the pattern confirmed that of Wilkins and Zubay[38]. However, there were several reflections not seen on the Wilkins and Zubay pattern which were interpreted as being possible reflections from the histone. They would probably constitute an α-helical configuration for the histone, and the histone would, then, lie parallel to the DNA molecule.

Despite the fact that the entire pattern was not obtained, a possible model was suggested for nucleohistone. This model was similar to that of Luzzati and Nicolaieff[20] for high concentration of DNH, but differed significantly from it in that the histone was ordered in the author's model, whereas there was no histone orientation in that of the former two authors. Both models are to be considered highly speculative.

More studies are necessary to elucidate the entire pattern. Solution of the Fourier Transform, a discussion of which was presented in the Introduction, is also necessary for models of DNH, and the calculated intensities from the model should be compared to those observed from the x-ray diffraction pattern. Indexing and intensities were not determined for the reflections on the film due to a lack of certain portions of the pattern.

The importance of water to the structure, and possibly to the function, of DNH was also discussed.

BIBLIOGRAPHY

1. Allfrey, V. G., Littau, V. C., & Mirsky, A. E. On the role of histones in regulating ribonucleic acid synthesis in the cell nucleus. Proc. Nat. Acad. Sci., 1963. 49, 414-421.

2. Bennett, H. S. The microscopical investigation of biological materials with polarized light. In R. McClung Jones (Ed.) McClung's handbook of microscopical technique. New York: Hafner, 1961. pp. 591-677.

3. Bernal, J. D. Structure arrangement of macromolecules. Discussions of the Faraday Society, 1958, 25, 7-18.

4. Bloch, D. P. On the deviation of histone specificity. Proc. Nat. Acad. Sci., 1962. 48, 324-326.

5. Bonner, J., & Huang, R. C. Properties of chromosomal nucleohistone. J. Mol. Biol., 1963. 6, 169-174.

6. Butler, J.A. V. The nuclear proteins of normal and cancer cells. Exp. Cell Res., 1963, Suppl. 9, 349-358.

7. Crick, F. H. C., Griffith, J. S., & Orgel, L. E. Codes without commas. Proc. Nat. Acad. Sci., 1957. 43, 416-421.

8. Cochran, W., Crick, F. H. C., & Vand, V. The structure of synthetic polypeptides. I. The transform of atoms on a helix. Acta. Cryst., 1952. 5, 581-587.

9. Cruft, H. J., Mauritzen, C. M., & Stedman, E. The nature and physico-chemical properties of histones. Phil. Trans. R . Soc., B, 1957, 241, 93-145.

10. Franklin, R. E., & Gosling, R. E. Molecular configuration in sodium thymonucleate. Nature, 1953. 171, 740-741.

11. Henry, N. F. M., Lipson, H., & Wooster, W. A. The interpretation of x-ray diffraction photographs. New York: St. Martin's Press, 1961.

12. Hidvégi, E. J., 'Arky, I., Antoni, F., & Várteresz, V. Studies on the heterogeneity and metabolic activity of histones from rabbit bone marrow cells. Brit. Cancer J., 1963. 17(2), 377-379.

13. Hnilica, L., Jones, E. W., & Butler, J. A. V. Observations on the species and tissue specificity of histones. Biochem. J., 1962. 82, 123-129.

14. Huang, R. C., & Bonner, J. Histone, a suppressor of chromosomal RNA synthesis. Proc. Nat. Acad. Sci., 1962. 48, 1216-1222.

15. Izawa, M., Allfrey, V. G., & Mirsky, A. E. The relationship between RNA synthesis and loop structure in lampbrush chromosomes. Proc. Nat. Acad. Sci., 1963. 49, 544-551.

16. Kendrew, J. C. The three-dimensional structure of a protein molecule. Scientific American, 1961, 205 (6), 93-110.

17. Kirby, K. S. A new method for the isolation of DNA's: evidence on the nature of bonds between DNA and protein. Biochem. J., 1957. 66 (3), 495-501.

18. Klug, A., & Franklin, R. E. Order-disorder transitions in structures containing helical molecules. Discussions of the Faraday Society, 1958, 25, 104-110.

19. Landridge, R., Wilson, H. R., Hooper, C. W., Wilkins, M. H. F., & Hamilton, L. D. The molecular configuration of deoxyribonucleic acid, I. x-ray diffraction study of the crystalline form of the lithium salt. J. Mol. Biol., 1960. 2, 19-37.

20. Luzzati, V., & Nicolaieff, A. The structure of nucleohistone and nucleoprotamines. J. Mol. Biol., 1963. 7, 142-163.

21. Mirsky, A. E., & Ris, H. The composition of isolated chromosomes. J. Gen. Physiol., 1951. 34, 475-491.

22. Nyburg, S. C. X-ray analysis of organic structures. New York: Academic Press, 1961.

23. Pauling, L., & Corey, R. B. Compound helical configurations of polypeptide chains: structure of proteins of the α -keratin type. Nature, 1953. 171, 59-61.

24. Pauling, L., & Corey, R. B. Specific hydrogen-bond formation between pyrimidines and purines in deoxyribonucleic acids. Arch. Biochem. Biophys., 1956. 65, 164-181.

25. Pauling, L., & Corey, R. B. The structure of hair, muscle, and related proteins. Proc. Nat. Acad. Sci., 1951. 37, 261-271.

26. Pauling, L., Corey, R. B., & Bronson, H. R. The structure of proteins: two hydrogen-bonded helical configurations of the polypeptide chain. Proc. Nat. Acad. Sci., 1951. 37, 205-211.

27. Perutz, M. F. Proteins and nucleic acids: structure and function. New York: Elsevier, 1962. pp. 3-59.

28. Phillips, D. M. P. The histones. Prog. in Biophys. and Biophys. Chem., 1962. 12, 211-280.

29. Rich, A., Davies, D. R., Crick, F. H. C., & Watson, J. D. The molecular structure of polyadenylic acid. J. Mol. Biol., 1961. 3, 71-86.

30. Sporn, M. B., & Dingman, C. W. Histone and DNA in isolated nuclei from chicken brain, liver and erythrocytes. Science, 1963. 140, 316-318.

31. Stedman, E., & Stedman, E. Cell specificity of histones. Nature, 1950. 166, 780-781.

32. Vendrely, R., Knobloch, A., & Vendrely, C. Données biochimiques recéntes sur la relation entre acide desoxyribonucleique et proteine basiques dans le noyau. Biochem, Pharmacol., 1960, 4, 19-28. (Abstract)

33. Watson, J. D., & Crick, F. H. C. Molecular structure of nucleic acids. Nature, 1953. 171, 737-738.

34. Watson, J. D., & Crick, F. H. C. The structure of DNA. Cold Springs Harbor Symp. Quant. Biol., 1953, 18, 123-131.

35. Wilkins, M. H. F. Physical studies of the molecular structure of deoxyribose nucleic acid and nucleoprotein. Cold Springs Harbor Symp. on Quant. Biol., 1956, 21, 75-87.

36. Wilkins, M. H. F., Gosling, R. E., & Seeds, W. E. Physical studies of nucleic acid; nucleic acid: an extensible molecule? Nature, 1951. 167, 759-760.

37. Wilkins, M. H. F., Stokes, A. R., & Wilson, H. R. Molecular structure of pentose nucleic acids. Nature, 1953. 171, 738-740.

38. Wilkins, M. H. F., Zubay, G., & Wilson, H. R. X-ray diffraction studies of the molecular structure of nucleohistone and chromosomes. J. Mol. Biol., 1959. 1, 179-185.

39. Wilkins, M. H. F., Zubay, G., & Wilson, H. R. X-ray diffraction studies of the structure of deoxyribonucleoproteins. Trans. Faraday Soc., 1959, 55, 497. (Abstract)

40. Zubay, G., & Doty, P. The isolation and properties of DNP particles containing single nucleic acid molecules. J. Mol. Biol., 1959. 1, 1-20.

41. Zubay, G., & Wilkins, M. H. F. An x-ray diffraction study of histone and protamine in isolation and in combination with DNA. J. Mol. Biol., 1962. 4, 444-450.

APPENDIX

CHEMICAL AND SPECTROPHOTOMETRIC ANALYSIS OF ZUBAY AND DOTY NUCLEOHISTONE EXTRACT

I. Chemical Analysis

A. Biuret Test for Protein
Sample size = 2.00 ml.
Absorption at 540m = 0.032 (estimated error of 3 - 4%)
Amount Protein in 2.00 ml. sample = 0.6 mgm.
Protein concemtration = 0.3 mgm./ml.
Protein N = 48 µg./ml.

B. Microkjeldal Analysis for Total(Protein and Base) Nitrogen
Total N = 83 µg/ml.

C. Nucleotide Nitrogen = 35 µg/ml. (83 µg/ml. - 48 µg/ml.)

D. Nucleotides on the average contain about 16.2% N by weight

Let x = µg nucleic acid/ ml.
Then 35 µg/ml. = 0.16x
219 µg/ml. = x (amount of nucleic acid in suspension)

E. From the Biuret test, the suspension contains 300 µg/ml. Therefore, the DNA/histone ratio is 0.73 by weight, and the suspension of DNH contains 42% DNA and 58% histone by weight.

F. Phosphate determinations were made, but were completely unreliable because of the incomplete acid hydrolysis of the nucleic acid.

II. Spectrophotometric Analysis
The ultraviolet spectrophotometric analysis between 220 mµ and 325 mµ gave the typical nucleohistone curve, with a maximum at 259 mµ and a minimum at 237 mµ. The optical density at 260 mµ was 0.827; at 280 mµ the optical density was 0.480. Dr. R. B. Lyons of the Department of Anatomy at the University of Oregon Medical School estimates that at an optical density of 0.4 at 260 mµ, the suspension contains approximately 20 µg DNA/ml. From E. Adams nomograph based on extinction coefficients for enolase and nucleic acid given by Warburg and Christian* nucleic acid concentration was estimated to be 35.2 µg/ml. in a 1:5 dilution of the original suspension. This value agrees fairly well with the value of approximately 40µg/ml. predicted by Dr. Lyons. Thus by Dr. Lyons estimate the nucleic acid concentration of the suspension is approximately 200 µg/ml.; from the nomograph it is 176 µg/ml. From the nomograph it is possible to estimate the protein concentration; however at nucleic acid concentrations of greater than 20% by weight, the spectrophotometric determination of protein is subject to considerable error, according to Warburg and Christian. The author believes that the Biuret and microkjeldal determinations are much more accurate for this suspension.

*Warburg, O., & Christian, W., Biochem. Z., 1942, 310, 384 - 421.

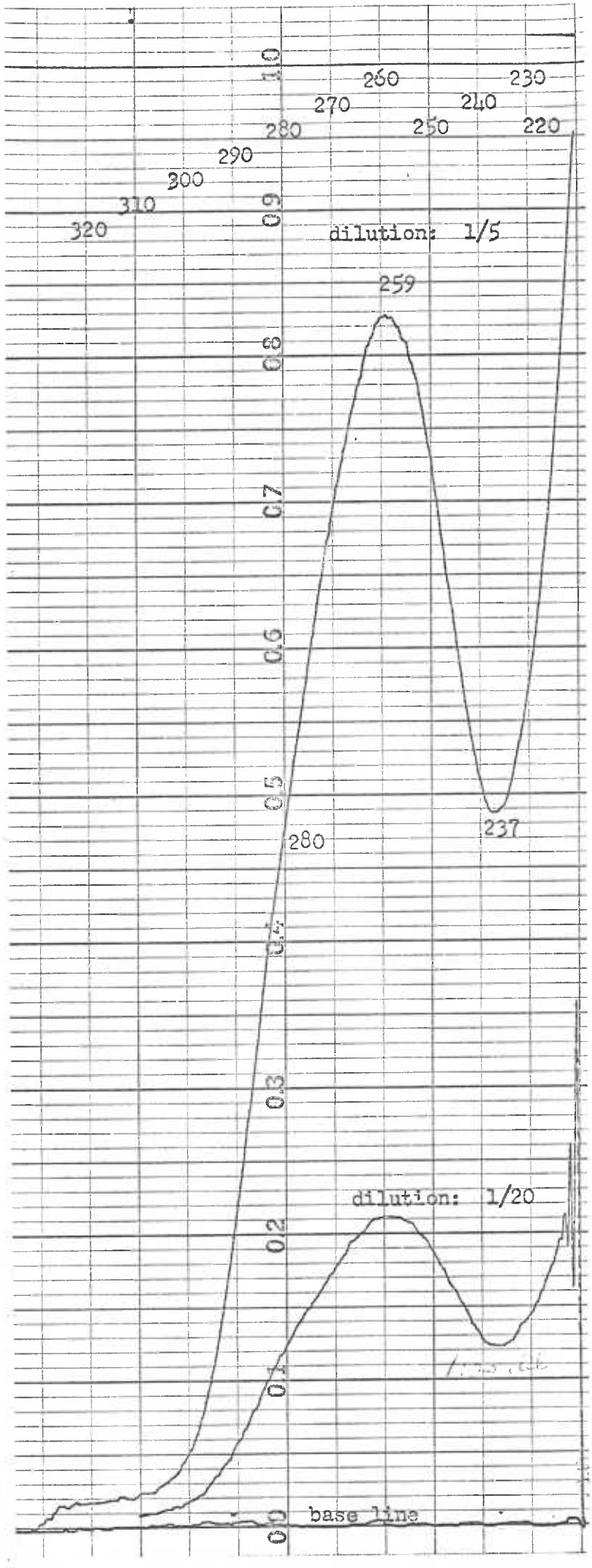
1.0
0.9
0.8
0.7
0.6
0.5
0.4
0.3
0.2
0.1
0.0
320
310
300
290
280
270
260
250
240
230
220
dilution: 1/5
259
237
280
dilution: 1/20
base line